ALBERT-LUDWIGS-UNIVERSITY OF FREIBURG

FACULTY FOR FOREST AND ENVIRONMENTAL SCIENCES

INSTITUTE OF HYDROLOGY

MSC. THESIS

Importance of the soil-rock-interface for surface water redistribution, infiltration and groundwater recharge on a semi-arid limestone slope

Author:

Jakob Sohrt

First examiner PD Dr. Jens Lange

Second examiner Dr. Heike Puhlmann

11. November 2012

Contents

List of Figures

List of Tables

List of Equations

1 Abstract

Infiltration characteristics in soil profiles neighbouring rock outcrops are determined through ten rainfall simulation experiments at two hillslopes in the mountain range east of Ramallah in the Westbank, Palestine. A precipitation event of 50 mm with an intensity of 20.61 $\mathrm{mm\,h^{-1}}$ on an area of 1 m^2 is conducted on each plot. The plot area is always overlaying the soil-rock interface at surface level so that 50 % of the plot share is located on the outcrop surface and 50 % on the adjacent soil. The runoff from the outcrop share is stained with brilliant blue FCF for optical identification of infiltration patterns.

An average of 17 hours after finishing the rainfall simulation, five cross-sections are dug at every plot along an axis perpendicular to the rock-soil interface at surface level. Soil moisture is measured on a 10 x 10 cm grid on every cross section with a UMS ML2x©-probe. In most cases it was not possible to stick to the aspired measurement density due to unfavorable soil conditions. Standardized photographs of every cross-section including a scale and a serial number are taken as well as soil samples on standardized locations. Runoff on the soil surface did not occur. The soil moisture measurements and photographs of cross-sections are used to generate continuous soil moisture data via universal kriging inside the geometry of each individual cross-section. It is discriminated between stained and unstained soil sections in order to calculate a separate soil water balance of water infiltration from the soil surface and water originating from the outcrop. The water balance is calculated using values of antecedent soil moisture measured individually for every precipitation experiment on a depth profile as close as possible to the respective plot. On average 77.8 % of the outcrop runoff is found to be percolating into the fractured bedrock compared to 36.6 % of the water infiltrating from the soil surface.

These datasets are used to calibrate a model which predicts the soil water balance as a function of soil depth and distance to the interface at surface level for every point on an axis perpendicular to the rock-soil interface at surface level. Since the creation of separate models for water originating from the outcrop and water originating from the soil surface was not successful there is no discrimination between these two groups in the model. The

model is calibrated on 1441 data points and validated on the remaining 805, reaching a Nash-Sutcliffe-Efficiency of 0.7, which was used as quality criterion. This model and other assumptions are used to predict the soil water balance along transects in Ein Samia and Kafr Malek where soil depth and proximity to the next rock outcrop is measured along seven transects with a total of 2200 points and a measurement density of 50 cm. The results of the model application show that percolation into the fractured bedrock is mainly due to runoff from outcrops and infiltration along the soil-rock interface (73% of the total water that percolates into the bedrock). Soil surfaces with no adjacent outcrop (distance $\succ$ 0.5 m) contribute only by about one third (27%).

The model is not capable of predicting recharge from actual precipitation data since it is calibrated for a single rainfall event of uniform magnitude and intensity. It serves more as a hint on how infiltration and groundwater recharge take place in the simulated precipitation event on a comparably high spatial resolution.

It was aspired to detect differences in soil-physical properties between two groups of soil samples. For one group the samples came directly from the soil-rock interface, for the other samples were obtained at locations 50 cm away from the interface. No significant soil physical differences have been found between both groups. In order to upscale the model results further it has been tried to relate surface properties like vegetation type or absence of such and proximity to outcrops with the soil depth for 2200 sampled points. No correlation between soil depth and the surveyed parameters has occurred.

2 Zusammenfassung

Zur Untersuchung der Bedeutung von partiell freiligendem Grundgestein in semi-ariden Hanglagen bezüglich der lokalen Grundwasserneubildung werden zehn Beregnungsexperimente durchgeführt. Die Experimente finden auf zwei Hängen westlich des Jordangrabens nahe bei Ramalla in der Westbank (Palästina) statt. Dabei soll ermittelt werden ob aufkommender Niederschlag, der von diesen Steinoberflächen abfließt, ein anderes Infiltrationsverhalten zeigt als Niederschlagswasser, dass direkt von der Bodenoberfläche aus infiltriert. Es wird postuliert, dass Abfluss von Steinoberflächen unterirdisch präferentiell abfließt und so im Mittel tiefer infiltriert und in größerem Umfang in das Grundgestein perkoliert, als Infiltration von einer reinen Bodenoberfläche. Es soll bestimmt werden, inwieweit dies zutrifft und welche Rückschlüsse daraus auf die lokale Grundwasserneubildung zu ziehen sind.

Die simulierten Niederschlagsereignisse betragen 50 mm und weisen eine Intensität von 20.61 $\mathrm{mm\,h^{-1}}$ auf, die Plotgröße beträgt 1 m^2. Der Plot wird dabei so platziert, dass 50 % auf einer freien Steinoberfläche liegen und 50 % auf angrenzendem Boden. Der aus der Beregnung resultierende Abfluss von der Gesteinsoberfläche wird mit Brilliant Blue FCF eingefärbt, damit diese Wasserfraktion später im Bodenprofil optisch identifiziert werden kann.

Im Mittel 17 Stunden nach Ende eines Beregnungsversuches werden auf dem Plot nacheinander fünf Bodenprofile aufgegraben. Die Profile sind nach einer Achse rechtwinklig zum Verlauf der Grenze von Boden und Grundgestein an der Oberfläche ausgerichtet. Auf diesen Profilen wird nach Möglichkeit in einem 10 x 10 cm Raster die Bodenfeuchte und auch die absolute Bodentiefe gemessen.

Diese Daten werden verwendet, um kontinuierliche, zweidimensionale Daten der Bodenfeuchte für jedes Bodenprofil mittels universal krigging zu erzeugen. In gleicher Weise wird eine flächenhaft aufgelöste Bodenwasserbillanz des simulierten Nierschlagsereignisses erzeugt. Die hierfür benötigte Vorfeuchte des Bodens wird für jedes Profil einzeln an einem möglichst nahe gelegenen Tiefenprofil bestimmt. Bei der Bilanzierung wird zwischen eingefärbten und nicht eingefärbten Flächenabschnitten unterschieden, um getrennte Wasserbillanzen zu

berechnen. Im Mittel 77.8 % des Abflusses der Steinoberfläche perkoliert durch Risse in das Grundgestein im Vergleich zu 36.6 % des Wassers, dass von der Bodenoberfläche aus durch die Bodenmatrix infiltriert.

Die Datensätze der flächenhaft aufgelösten Wasserbillanzen werden verwendet, um ein empirisches Modell zu kalibrieren. Dieses prognostiziert bei gegebener Bodentiefe und Entfernung vom nächsten freiliegendem Grundgestein den Teil eines 50 mm Niederschlagsereignisses, der bis ins Grundgestein infitrtriert und so als potentielle Grundwasserneubildung zur Verfügung steht. Das Modell wird an 1441 Punkten kalibriert und an den verbleibenden 805 validiert. Die Nash-Sutcliffe-Efficiency für den Vergleich von Modell- und Messwerten beträgt 0.7. Dieses Modell und andere Annahmen werden verwendet, um entlang von Transekten, an denen Bodentiefe und Entfernung zum nächsten freiligendem Grundgestein gemessen wurde, die potentielle direkte Grundwasserneubildung nach einem exemplarischen Niederschlagserieignis zu berechnen.

Die Ergebnisse sowohl der Bodenfeuchtemessungen als auch der Modellanwendung zeigen, dass blanke Steinoberflächen für die Umverteilung von auftreffendem Niederschlag und dessen Versickerung in das verwitterte Grundgestein auf den untersuchten Hängen von großer Bedeutung sind. Dem Modell nach erzeugen Steinoberflächen und die Bodenmatrix in der direktem Umgebung ($\prec$ 0.5 m) 73% der potentiellen direkten Grundwasserneubildung, Bodenoberflächen weiter entfernt von freiligendem Grundgestein nur 27%, obwohl letztere Gruppe einen größeren Flächenanteil einnimmt.

3 Introduction

Groundwater recharge in semi-arid and arid environments is difficult to determine and highly variable depending on ambient conditions. Average precipitation alone is no sufficient basis for estimations of groundwater recharge: In an arid karstic aquifer in Saudi-Arabia, for example, about 47 % of the average precipitation of 70 mm a^{-1} contributes to groundwater recharge (Hötzl, 1995). This relatively high recharge is due to the favorable surface conditions where widely exposed limestone bedrock promotes quick infiltration through cracks and sinkholes. The existence of a soil layer and/or plant cover can reduce recharge significantly through water retention and evapotranspiration. This is illustrated by Leduc et al. (1997), who determined an average recharge of 50-60 mm a^{-1} in a semi-arid area in Niger with an average precipitation of 500-600 mm a^{-1}.

Differences in soil-physical and plant-physiological properties pose an important influence on point-scale groundwater recharge as Finch (1998) pointed out with a sensitivity analysis on the parameters of a recharge model applied in Great Britain.

The area the following study takes place in is situated on the eastern slope of the Judean Mountains dividing the eastern and western aquifer underlying the Westbank, Palestine. Groundwater recharge in this area has recently been estimated through differences between precipitation and spring discharge, pumping activity and groundwater fluctuation (HWE, 2010 in Hanf, 2010) as well as the use of flow models (Weiss & Gvirtzman, 2007) and tracer studies (Ayalon et al., 1998). These studies, however, focus on average recharge integrated over large areas. The spatial heterogeneity of recharge due to differences regarding geomorphology, soil type, geology, and land use is hardly taken into account.

Infiltration on slopes such as the experimental sites, which are characterized by frequent rock outcrops, tends to be spatially inhomogeneous due to the large variability in hydraulic conductivity of the surface components. Soil patches allow infiltration of incoming precipitation while rock outcrops generate surface runoff which is redistributed to the surrounding soil. There is the possibility of preferential flow-paths on soil-covered rock surfaces, either through subsurface erosion or due to the swell-and-shrink-behavior of the adjacent soil depending on its current state of moisture.

Experimental research regarding the importance of rock-soil interfaces for the vertical component of preferential flow could improve the understanding of infiltration, groundwater recharge, and runoff generation from slopes with frequent rock outcrops. Extensive research has been carried out regarding the importance of the rock-soil interface for lateral flow of water at the hillslope scale (Bockgard & Niemi, 2004; Freer et al., 2002; Mcdonnell, 1990; Roy et al., 2001, Tani, 1997; Weiler & McDonnell, 2003). However, the effect of the soil-rock interface regarding net vertical percolation has been studied less, even though it may be important for groundwater recharge under semi-arid and arid conditions.

Studies in semi-arid areas about the effect of discrete stones on infiltration have been summarized by (Wilcox et al., 1988). The included studies show a positive correlation of stone cover and infiltration due to the fact that the stones provide protection from splash erosion and surface sealing. Poesen et al. (1990) show that the direction of the correlation depends on whether the rocks lay on the soil surface or are embedded in the soil. In the latter case, a negative correlation of stone cover and infiltration rate was reported because of a reduction of the surface fraction where infiltration can take place. Experiments by Abrahams & Anthony (1991) found vegetation-induced effects to be dominating infiltration patters on a semi-arid slope in Arizona regardless of stone cover. It remains unclear if the results from these studies, which were partly obtained from laboratory experiments, can be applied to the area this study takes place in. Additionally, it can be assumed that the effects of the rock-soil interface on small discrete stones are different from the interface on a bedrock surface. Also, infiltration into the soil is not necessarily connected to groundwater recharge since a large fraction of soil water is lost to evapotranspiration under semi-arid conditions.

The rainfall response of slopes in Israel and Palestine is known to be quite variable depending on rainfall intensity and the surveyed scale. During 12 small-scale rainfall simulations with an intensity of 45 - 40 mm over the course of one hour by Cerd'a (1998), runoff occurred in only three cases. It needs to be stated that the experiments by Cerd'a (1998) were conducted exclusively on soil-covered surfaces.

Lange et al. (2003) conducted a large-scale precipitation experiment with a magnitude of 96,8 mm over the course of two days on a 180 m plot in the Carmel Mountains, Israel. Extensive runoff from the plot was observed already halfway through the experiment. Discontinuous runoff from the partly rock-covered sections of the plot occurred much faster but faded in soil pockets. The percolation rate into the bedrock was found to be 2.6 - 3 $\mathrm{mm\,h^{-1}}$. After the saturation of the plot, 80 % - 90 % of the applied precipitation contributed to runoff. Parameter values of the percolation rate into the bedrock are scarce and the permeability of the soil layer and bedrock material can be assumed to be highly variable as a response to differences in climate, geology, and land use.

Yair (1983) recorded continuous surface runoff in a rainfall simulation in the Negev Desert, Israel, with a magnitude of 30 mm, carried out in three pulses over the course of three days. The experimental slope consisted of upslope areas dominated by rock outcrops and increasingly thick colluvial soils downslope. Runoff from the widely exposed bedrock upslope was produced almost instantly after the sprinkling started which infiltrated completely in the colluvial soil downslope. Continuous runoff over the whole slope occurred after the third precipitation pulse.

The quick runoff response of outcrop surfaces observed by Yair (1983) and Lange et al. (2003) raises some interesting questions. It is still unclear how this runoff is distributed to the surrounding soil. Depending on the saturated conductivity of the soil it might either infiltrate directly along small-scale flow paths until reaching the bedrock, or successively exceed the infiltration capacity of the topsoil causing it to infiltrate over a larger area. The clarification of this issue poses an interesting task since the fraction of water reaching the below-ground bedrock material can be seen as potential groundwater recharge.

Research regarding the generation of surplus water in soil sections neighboring soil-rock interfaces in response to outcrop-runoff and the below-ground flow patterns of this water might lead to a significant improvement of the understanding of the fine-scale variability of infiltration and, thus, groundwater recharge. Especially in regions where water supply is sparse, information on spatial variability of recharge and dependence of such on certain surface- and soil properties can be helpful regarding process-based modeling and a sustainable management of land and water.

The aim of this study is to determine the importance of the soil-rock interface for redistribution and vertical percolation of incoming precipitation water. This serves to identify the local processes responsible for percolation of water below the soil layer and thus, potential groundwater recharge.

4 Site Description

Both experimental slopes are located close to Ramallah on the eastern flank of the Judean Mountains in Palestine, close to the village Kafr Malek and the Ein Samia well house. Their difference in altitude and location is reflected in the average rainfall, yielding on average 315 mm a^{-1} in Ein Samia and 466 mm a^{-1} in Kafr Malek during the last three years (see fig. 4.1). The two experimental slopes also vary in terms of aspect, inclination, surface cover, and underlying bedrock material. The site Ein Samia was mainly selected because of previous measurements at this location by Hanf (2010) including infiltration rates and soil-physical properties. The slope is especially beneficial since it covers six different strata (see fig. 4.3.2) and various surface cover types. The slope in Kafr Malek was selected because it features different properties in terms of soil thickness, vegetation, and inclination. It also needs to be taken into account that the difference in average precipitation might influence the formation of preferential flow paths.

4.1 Soils

Rendzina and Terra Rossa are recorded on the slopes within the study sites (Dan & Raz, 1970), which is confirmed for the study site of Ein Samia in a recent study by Hanf (2010). Since both soil types share some physical characteristics and grade into each other, it can be difficult to distinguish between them (Singer, 2007). The amount of undissolved carbon, however, may help to discriminate between the two soil types since Terra Rossa soils are usually free of it, as opposed to Rendzina soils (Singer, 2007; Blume et al., 2010).

A variety of explanations regarding the genesis of Terra Rossa soils can be found. They might be Paleosols (Horowitz, 1979), formed under present conditions (Yaalon et al., 1966) or originate from aeolian deposits of Sahara-dust (Muhs et al., 2010; Rapp, 1983). Terra Rossa soils usually have a high clay content of 60 - 70 % (Singer, 2007) which indicates a high water retention capacity.

Rendzina soils originate from chemical and physical weathering of different kinds of limestone, dolomite, and gypsum. The soil consists mainly of silicates, oxides, and undissolved particles of the parent material. The high clay content in the topsoil is reflected in a high water retention capacity (Blume et al., 2010).

4.2 Precipitation

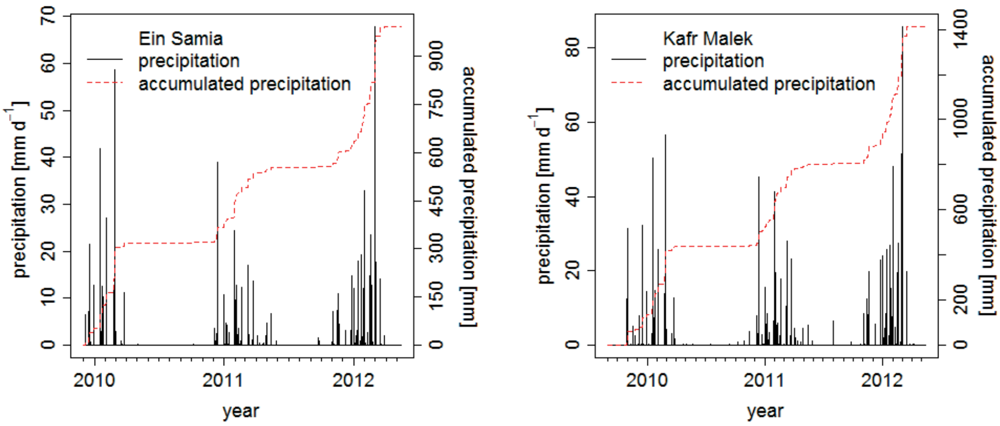

Figure 4.1: Precipitation in Ein Samia and Kafr Malek for three raining seasons in daily resolution

Precipitation data for the study sites is only available for three rain seasons, the next long-term record coming from a station in Ramallah. Since temporal distribution and amount of precipitation can be assumed to be variable along the elevation gradient from Ramallah to the study sites the Ramallah rainfall record is not used in this thesis.

Precipitation occurs mainly between November and March, almost no rain is recorded in the summer months. Even though the temporal pattern of rainfall events is very similar on both sites, Kafr Malek receives a considerable surplus of water (see fig. 4.1). While low-magnitude events of 10 mm or less are by far the most frequent, they account for only about 23 % of the total precipitation height (see tab. 4.1). Rainfall events above 40 mm d^{-1} occur regularly on both sites and contribute considerably to total precipitation.

4.3 Ein Samia

The NNW-exposed slope on which the experiments take place is located at the coordinates N 31° 59.056, E 35° 20.471 and stretches from 409 m to 474 m above sea level. The slope angle is mainly uniform and mostly diminishing towards the hilltop. Steeper sections with widely exposed rock are found on the eastern part of the slope (see fig. 4.2). Many features

Table 4.1: Frequency and magnitude of precipitation events in Kafr Malek and Ein Samia with: Classes [mm], Ev. quant. = Event quantity, Acc. prec. = Accumulated Precipitation [mm], Frac. tot. = Fraction of total precipitation [%]

	Ein Samia			**Kafr Malek**		
Classes	Ev. quant.	Acc. prec.	Frac. tot.	Ev. quant.	Acc. prec.	Frac. tot.
0 - 10	129	227.4	22.92	161	303.51	22.88
10 - 20	35	313.2	31.57	44	366	27.59
20 - 30	12	96.2	9.69	20	225.98	17.03
30 - 40	8	141.2	4.23	11	137.76	10.38
40 - 50	4	87.6	8.83	7	134.67	10.15
$\succ$ 50	2	58.6	5.90	4	158.4	11.94

of the slope correspond to intensive grazing from sheep and goats, for example trails and damage to perennial plants. The valley floor is filled with colluvial sediments of unknown depth, covering several hectares. Since fertile farmland is scarce in this area, most of it is irrigated for crop production.

4.3.1 Surface types

Bare rock and annual plants cover most of the area; fewer parts are occupied by shrubs, bare soil, and gravel. The shrub-layer mainly consists of *Poterium spinosum* (Syn. *Sarcopoterium spinosum*), perennial plants with a height above 30 cm are extremely rare. The occurring annual plants grow and reproduce in the rain season and lay dormant as seeds in the dry period. Perennial plants outlast in bulb form or stay partly active during the dry season, which applies for the shrub layer. Artifacts of former settlement and cultivation of the land are present all over the slope. Leftovers of terraces cover the less steep parts, large ruins and extensive burial grounds are found towards the hilltop as well as quarry. Considering this it can be assumed that the distribution of soil on this slope has been heavily influenced by land management.

Rock outcrops occur scattered or aligned in banks parallel to the slope. Such banks occur increasingly in the north-eastern and upper part of the slope.

4.3.2 Geology

Seven different strata are present in the study area which contain different limestones from the upper cretaceous. The valley floor is covered with quaternary sediments. Multiple fault-lines are present in the study area (see fig. 4.3.2). The transitions of the strata as well as

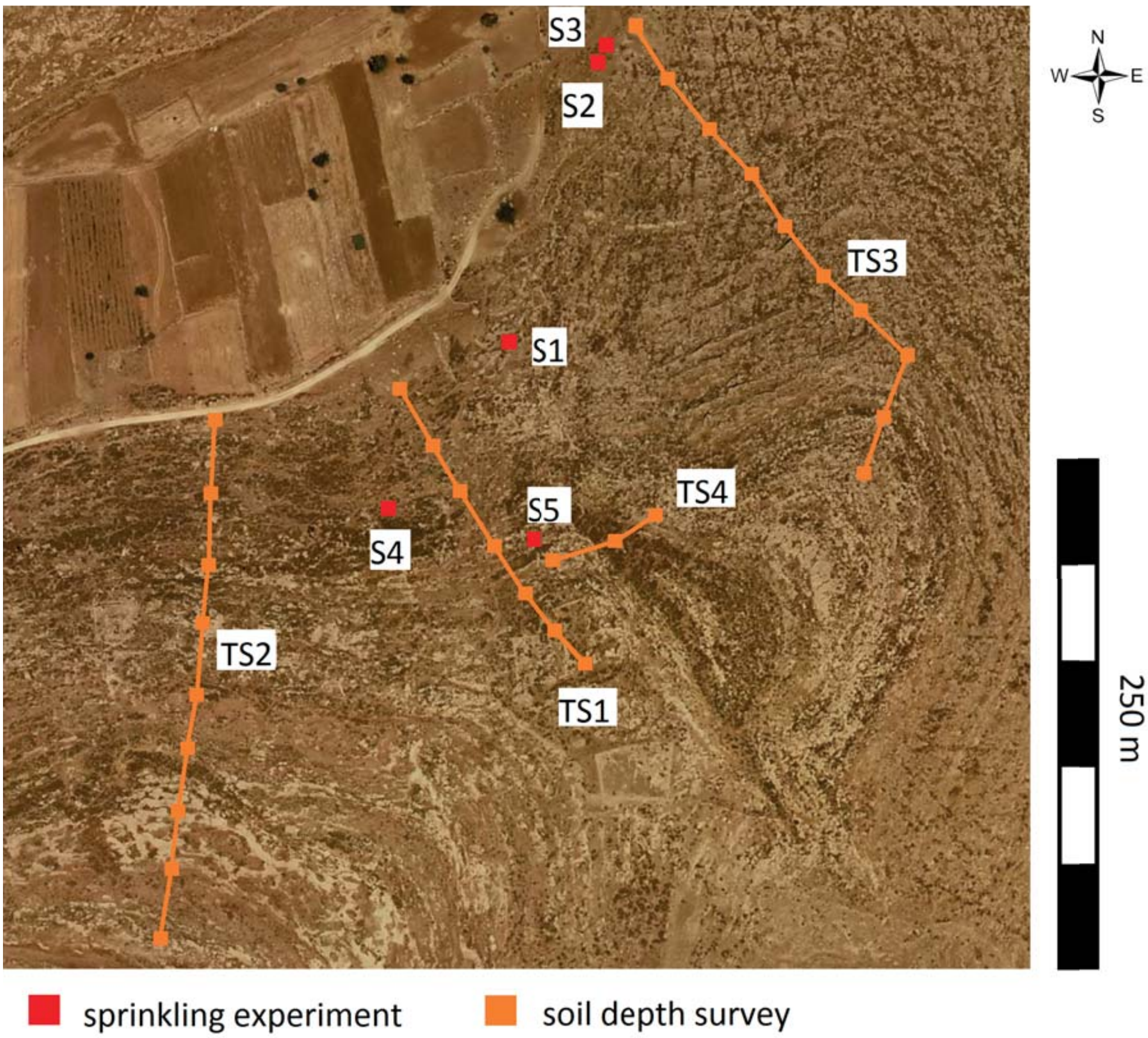

Figure 4.2: Aerial photo of the experimental slope close to Ein Samia. Photo: Israel Map Survey, 2009

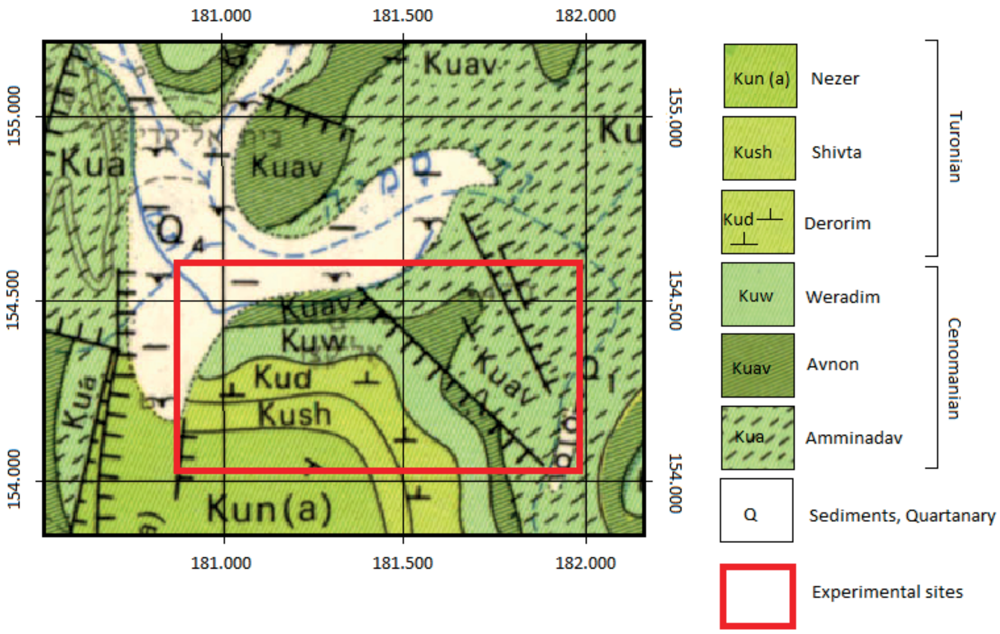

Figure 4.3: Geological Map of Ein Samia, coordinates according to Israeli Grid. Modified after Begin (1974)

the fault lines are mostly visible mostly to the naked eye (with a fuzziness of several meters). Shivta and Nezer represent hard limestone strata which are dissolved rather slowly, whereas Deronim and Weradim are more clastic, which promotes weathering. The Amminadav-formation is built out of dolomite which dissolves slowly but features frequent cracks. The lowest strata toward the valley floor is composed of Avnon, a soft and marly limestone (Begin, 1974).

It is notable that hillside cuts and historic caverns give insight into the uppermost geological structure of the slope. Frequent soil intrusions inside the bedrock with an aperture of several decimetres are found frequently until at least 150 cm below the soil layer. This is confirmed for the hillside toe and the middle slope.

4.4 Kafr Malek

The study site of Kafr Malek on an ESE exposed slope is located at the coordinates N 31° 59.919, E 35° 17.873. Experiments take place between 737 m and 814 m above sea level. Slope aptitude ranges from extremely steep at the hilltop to moderate at the hillside toe. Olive groves are scattered in the middle slope (see fig. 4.4), grazing only occurs on the lower part of the slope. Signs of repeated fire clearance have been observed. Relicts of former cultivation on the now barren parts of the slope occur on a regular basis but not as densely as in Ein Samia. Still it is assumed that especially olive cultivation led to soil displacement and disturbance in the past.

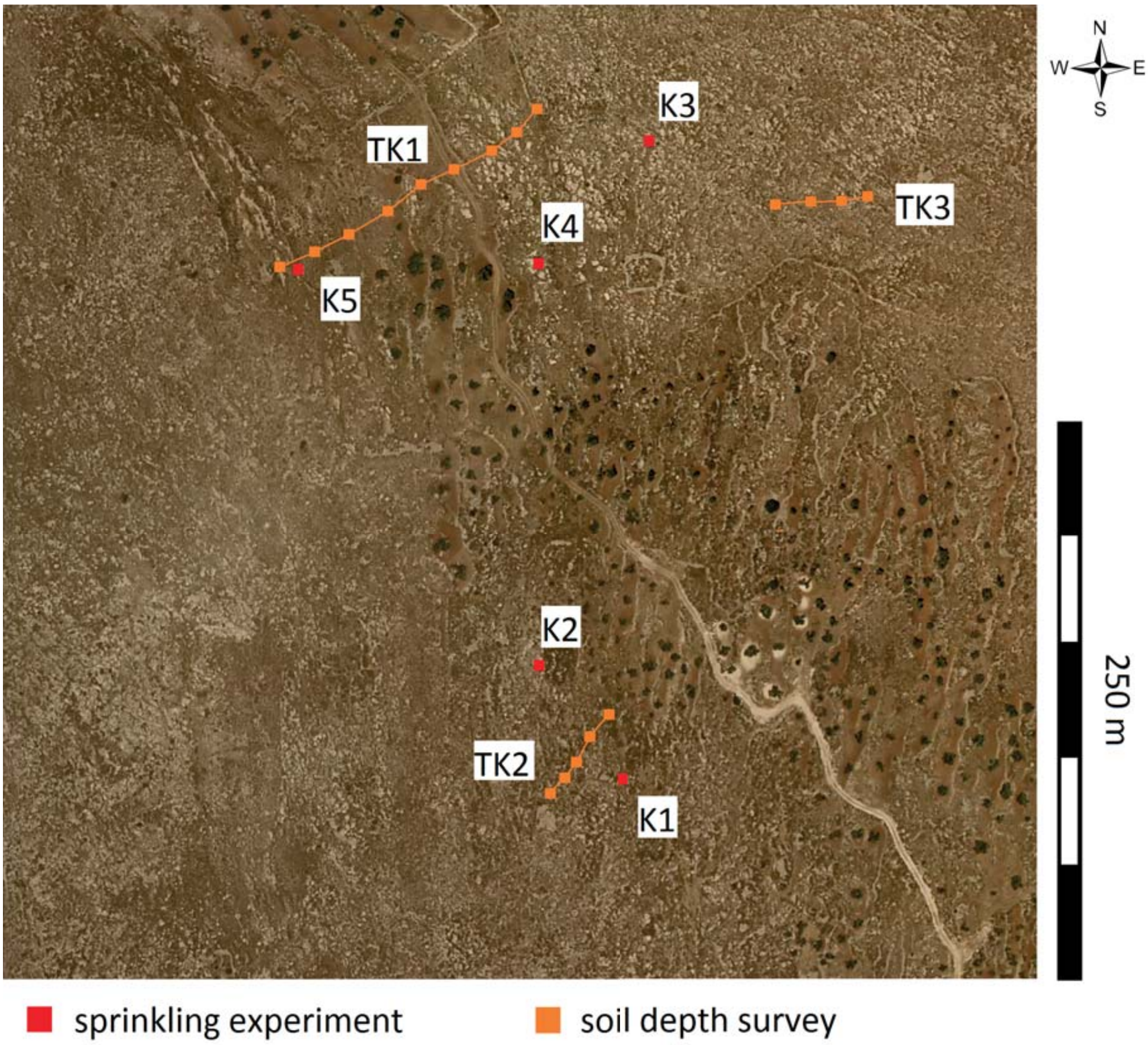

Figure 4.4: Aerial photography of the experimental slope close to Kafr Malek. Photo: Israel Map Survey, 2009

4.4.1 Surface types

Most of the experimental site is covered with *Poterium spinosum* and other perennial plants even though plants exceeding 30 cm in height are extremely rare and only found in the steeper parts towards the hilltop. This native tree vegetation consists mainly of *Quercus ilex*. Annual plants increase progressively towards the hillside toe. Still a large area fraction is occupied by rock-outcrops. Rocks of few decimetres up to a meter in size are found frequently on ore embedded in the soil surface with no connection to the bedrock. Considering this and the very steep upslope conditions it should be taken into account that the material on the experimental slope could be partly the result of hillside slumping. Another hint in this direction is the fact that the alignment, size, and height/steepness of rock outcrops are rather chaotic, compared to the slope in Ein Samia. Aligned outcrops along the stratification are only found at the steep upslope. Since the present dolomite gets dissolved rather slowly the origin of present characteristics and distribution of rock-outcrops is probably due to mass displacement rather than in-situ dissolution of ambient bedrock.

4.4.2 Geology

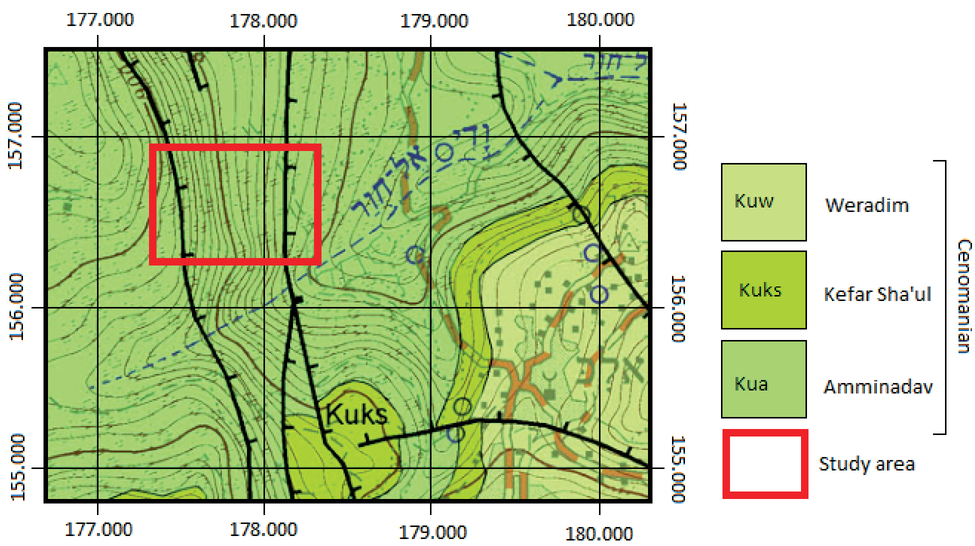

Figure 4.5: Geological map of the experimental site close to Kafr Malek, coordinates according to Israeli Grid. Modified after Shachnai (2000)

The only stratum present in the study close to Kafr Malek is Amminadav, a hard dolomite limestone from the upper cretaceous (see fig. 4.5). All plots are located in between the two fault lines.

5 Method

5.1 Rainfall Simulation

5.1.1 Setup

The rainfall simulation device consists mainly of three parts: the sprinklers, the pump, and the wind protection. Four Gardenia MicroMist© nozzles are used as sprinklers. Whilst their droplet spectrum is very fine when using the recommended working pressure of about 2 bars much larger droplets are produced using a lower working pressure. The nozzles are placed in the corners of a 1.6 x 1.6 m square, pointing upward towards its center with a vertical tilt of 38 °. The four nozzles are interconnected by a hosepipe with an inner diameter of 8 mm. This hosepipe is arranged in a circle. This is meant to reduce the risk of pressure differences within the hosepipe by allowing water supply from two directions for every nozzle. The circular hose that is attached to the nozzles is connected with the pump with an interposed pressure gauge. The reading of the pressure gauge is the reference parameter for the flow of water through the nozzles.

As for the pump, a Shurflo 8000-443-136© is used. The flow rate of the pump is controlled using a Kemo Power Controll M171© potentiometer which can be used to level the input voltage to the pump. Both units are connected to a radiator grill with active air-cooling and fitted in a metal suitcase to provide sufficient stability for outdoor use at high ambient temperature. A stainless-steel filter with an 0.3 mm aperture width is built in upstream of the pump to avoid clogging of the pump and nozzles.

The input voltage to the pump for any given switch position of the potentiometer can vary due to battery charge, ambient temperature, and other influences. The reading of the pressure gauge, however, provides a distinct reference parameter. Therefore, the reading of the pressure gauge is used as reference parameter for the flow of water through the nozzles. The correlation between these two variables is established through manual calibration.

Due to the heterogeneity of the micro-topography around the plot the nozzles are placed on a wooden frame. The height of said frame above ground is adjusted in order to have all nozzles on a levelled surface. This is conducted either by attaching the frame with string to the inner frame of the tent or by placing it on adjustable legs. The evenness of the frame is verified by measurements with an air level before each experiment. The pressure gauge is always attached at the same height as the nozzles to ensure accurate pressure readings.

The whole construction is placed inside a 3 x 3 m tent to avoid disturbance of the rainfall distribution due to wind influence while, at the same time, allowing access to the operation site (see fig. 5.1).

During the whole experiment brilliant blue FCF is applied to the outcrop-share of the plot. It is distributed manually using a 60 ml shot every 5 minutes. The concentration of the applied solution is 100 $\mathrm{g\,l^{-1}}$. Assuming that the stone fraction covers about 50 % of the respective plot the color gets diluted to 4 $\mathrm{g\,l^{-1}}$ through the supply of the artificial rainfall on the rock surface. According to Gjettermann et al. (1997), Germán-Heins & Flury (2000) and Weiler & Flühler (2004), this concentration leaves room for considerable dilution underground without the danger of the dye patterns fainting.

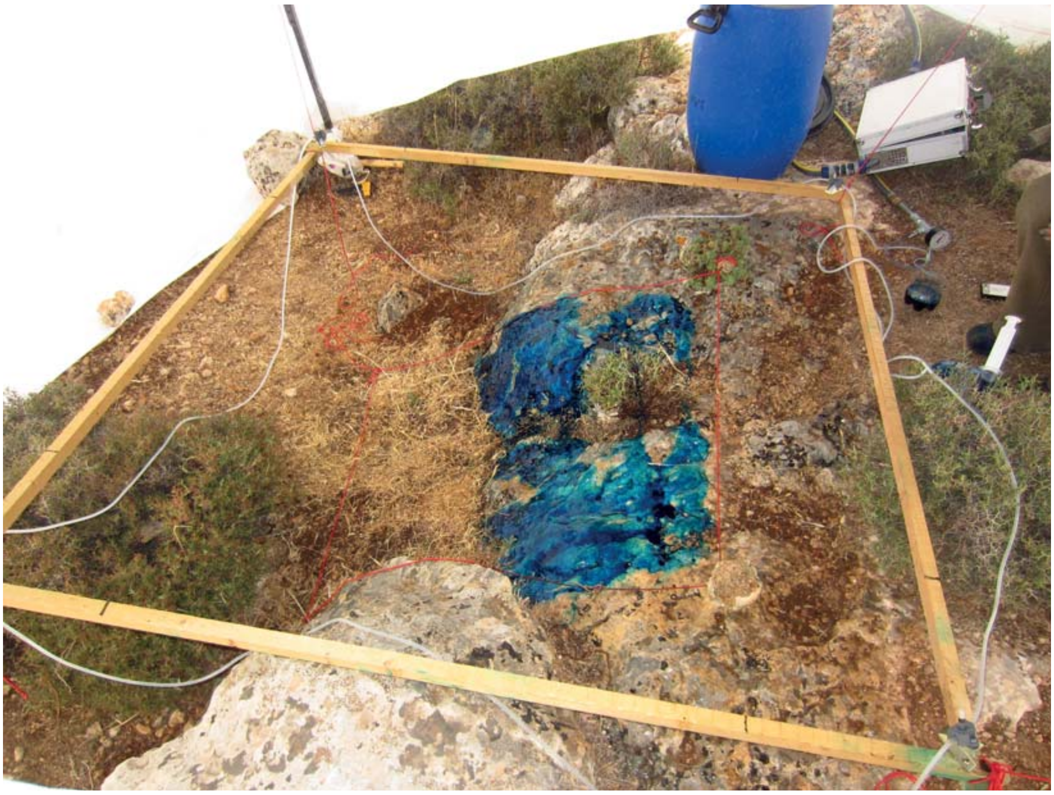

Figure 5.1: Rainfall simulation in progress. Red thread is used to mark the plot outline. The barrel in the back contains the water; the suitcase next to it holds the pump, battery and power control device. Foto: Fabian Ries

5.1.2 Calibration

The calibration of the rainfall simulator is carried out under windless conditions. The uniformity of the rainfall distribution is measured using an array of 36 cups which were set up in a 20 x 20 cm matrix, thereby covering a total area of 1 m^2. The Christiansen Coefficient (Christiansen, 1943) is used as criterion to describe the uniformity of water retention in the cups, which is measured every 30 minutes. Since the sprinklers are mounted on a plane array, while the irrigated area can be rough, two series of sprinkling experiments are carried out for calibration. The sprinklers are placed at surface level for the first and 50 cm above surface level for the second experiment.

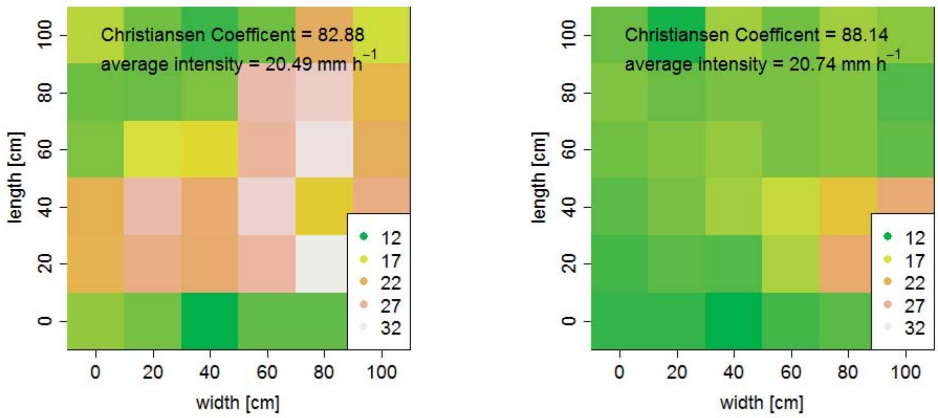

Figure 5.2: Spatial distribution of water in the cups for experiments carried out in zero respective 50 cm height. Each series consists of four sprinkling experiments lasting 30 minutes each

The most uniform distribution of simulated rainfall was produced at a water pressure of 0.66 bars resulting in a precipitation intensity of 20.615 mm d^{-1}. A more uniform distribution of the simulated rainfall is achieved by placing the nozzles 50 cm above the surface (see fig. 5.2), though even when the nozzles are placed at surface level the Christiansen Coefficient is still within an acceptable range. Since a higher installation of the nozzles increases the vulnerability to wind influences, which could not be totally eliminated by the tent, the nozzles are always placed on a plane which intersects with the highest point of the plot.

5.2 Simulated Rainfall intensity

It is aspired to simulate a precipitation event of 50 mm. Events of 50 $\mathrm{mm\,d^{-1}}$ occur on a regular basis in Ein Samia as well as in Kafr Malek, even though they are on the upper end of the occurring range of rainfall events (see fig. 4.1). A relatively intense precipitation event is chosen for the experiments since their limited number does not allow for the simulation of multiple rainfall intensities. Ayalon et al. (1998) and Owor et al. (2009) suggest that the amount of recharge in semi-arid environments is mainly driven by high-intensity precipitation events exceeding a site-specific threshold. Avner et al. (1998) studied a catchment in central Israel and concluded that rainfall events $\prec$ 20 mm are mostly lost due to evaporation and do not contribute to groundwater recharge.

Given that existence and specification of such a threshold are unknown for the study sites, a rainfall intensity from the upper end of the occurring range is picked for the experiments. A sprinkling duration of 145.5 minutes at an intensity of 20.615 $\mathrm{mm\,h^{-1}}$ results in a total simulated rainfall of 50 mm.

5.3 Recharge determination approach

Determination of groundwater recharge is no trivial task. In this approach, only direct recharge is taken into account. Direct recharge is defined as the fraction of precipitation that exceeds the retardation capacity of the soil and reaches the ground water table via direct vertical infiltration (Lerner, 1997). Direct recharge can be determined either by direct measurement with lysimeters, via soil water balance, tracer application, or by process based and empirical models (Stephens, 1996).

In this thesis, a combination of soil water balance approach and empirical modelling is used. Infiltration properties on soil surfaces and transition zones of soil and rock outcrops on the surface are determined via rainfall simulation and high-resolution soil moisture measurement. The spatially resolved soil water balance is derived from the deviation of antecedent soil moisture, which is measured in the closest possible location for each plot individually, and the measured soil moisture after the sprinkling experiment. The resulting soil water balance is reviewed for special dependency on the soil-rock interface. An empirical model is fitted to represent this dependency and used to predict the soil water balance on a larger scale. It is assumed that water percolating below the soil layer and into the bedrock contributes to groundwater recharge.

5.4 Below-ground flow velocity

Five soil moisture probes (Decagon 5MTE/M) are installed in cross-section K3-1 prior to the rainfall simulation. Three probes are installed directly at the soil-rock interface in depths of 10, 30, and 40 cm. The two other probes are installed in depths of 10 and 30 cm, respectively, in a horizontal distance of 20 cm to the interface. This setup is designed to compare the flow velocity of vertical matrix infiltration and possible preferential flow along the interface. The reading of the probes close to the interface cannot be interpreted as actual volumetric soil moisture since it is influenced by the neighbouring rock. It serves only to compare how long it takes for the infiltration front to reach a certain depth.

5.5 Soil moisture measurements

Except for plot K3, five cross sections are dug perpendicularly to the interface at surface level for every plot site 10, 30, 50, 70, and 90 cm from the plot border. The digging of the profile takes place an average of 17 hours after the end of the sprinkling experiment. It is aimed to dig the cross-sections until reaching the bedrock. Each cross-section is photographed with a scale and a note displaying location and serial number. A UMS ML2x©-probe is used for the measurements of the soil water content. It is aspired to take measurements every 10 x 10 cm, which is not always possible due to extremely compact/loose soil and frequently high gravel content. The depth of the soil profile is recorded every 10 cm along at each cross-section.

5.6 Soil particle size and organic carbon content analysis

Bulk soil samples are collected at 13 locations, including the experimental plots. One sample is always collected directly from the surface of the interface from a depth of 10 cm, while another is collected at a distance of 50 cm perpendicular from the interface at surface level, equally from a depth of 10 cm. The purpose of this is to compare these two groups of samples regarding their particle size distribution and organic carbon content. Since it can be reasonably assumed that the rate of soil evolution in semi-arid conditions is mainly limited by water availability this analysis is meant to test the conclusions of soil water distribution derived from the sprinkling experiments. Cooley (2002) pointed out that relatively high clay fractions can be expected along preferential flow-paths on limestone geology. The soil organic carbon content serves as proxy for the density of (former) tender roots, which in turn serve as proxy for average soil water availability.

The samples are packed in airtight and lightproof bags and stored in a cool environment. They are then placed in a drying oven over the course of three days with ambient temperature of 35 °C. During the drying, the samples are repeatedly ground by hand in order to prevent aggregate formation. This relatively laborious method is necessary to avoid destruction of partly weathered limestone particles and, thus, corruption of the particle size analysis. Aliquots for the organic carbon content and the particle size analysis are removed from the bulk sample.

The particle size analysis is performed using the Köhn-pipetting-method (DIN ISO 1127, 2002) The aliquot is tested for undissolved limestone particles by adding a small amount of sulphuric acid. The aliquot is then placed in an Erlenmeyer's flask on a charfing dish and admixed with H_2O_2 in order to destroy the organic content. H_2O_2 is applied until gas release from the sample comes to a halt. The resulting water content is continuously vaporized by heating the sample to temperatures $\preceq$ 80 °C. A $Na_4P_2O_7$ solution is applied as a dispersion agent. The sample is placed in a sedimentation flask which is then filled with distilled water. The flask is stirred through agitation to dispense the sample in the water. Samples are extracted by a pipette from a distinct depth at distinct times. The settling velocity of a globular body in a (fluid) medium can be calculated using Stokes' law (see eq. 5.1):

$$v = \frac{2}{9} \cdot \frac{\rho_{body} - \rho_{medium} \cdot r^2 + g}{\eta} \tag{5.1}$$

Stokes' Law with: v = settling velocity [m s^{-1}], ρ_{body} = density of floating particle [kg m^{-3}], ρ_{medium} = density of medium[kg m^{-3}], r = radius of the particle[m], g = gravitational acceleration [m s^{-2}], η = viscosity of the medium [Pa s]

Thus, the maximum radius of particles present in a distinct depth of the cylinder at a given time can be calculated. This is used to determine a depth/time ratio in order to collect aliquots containing particle sizes according to DIN 4022 (1987). The aliquots extracted by pipette are released into a petri-dish which is placed in a drying oven at 105 °until the water fraction is evaporated. The aliquots are then weighed with a high-definition scale.

The fraction of particles with a diameter of $\succ 0.063$ mm is determined by wet sieving. The soil organic carbon content is measured with a combined effort of the Woesthoff apparatus and a mass spectrometer. The first is used to determine the amount of anorganic carbon, while the latter measures the amount of total carbon. The difference of the two values accounts for the soil organic carbon.

5.7 Soil depth survey

The average soil depth along the slope in the two study areas is determined using a 1.2 m steel probe which is piled in the soil using a sledgehammer. Measurements are taken every 50 cm at linear transects, mostly along the dip line of the slope. Every 25 m position and height are determined using a Garmin GPSMap 76 CSX©. The placement of the transects is determined in order to cover the area used for rainfall simulation in terms of maximum and minimum height as well as width along the slope. Additionally, it is aspired that all geological formations and different types of vegetation are cover. The transects are documented with high-resolution photography and an adjacent scale which allows for the identification of every survey point with an accuracy of a few centimetres within the photo. Each measurement point is classified according to the surface cover types 'bare stone', 'bare gravel', 'bare soil', 'annual plant cover' and 'perennial plant cover'. Additionally, the distance from each surveyed point to the next rock-soil interface is measured. The purpose of this survey is to find possible correlations between surface cover types, distance to the next soil-rock interface, and soil depth. This could be used to estimate the soil depth from aerial images and thus to upscale the results of the study beyond the surveyed transects. A total of 1422 points are probed in Ein Samia and 758 in Kafr Malik.

5.8 Mapping of surface runoff

Signs of the occurrence of concentrated surface runoff on rock surfaces are only present in the study area of Ein Samia. In some cases this is due to the weathering of a small 'channel' into the rock surface or a sudden change in color along a flow line compared to those parts of the rock surface that stick up (see fig. 6.11).

The mapping of said characteristics is carried out in a rather qualitative way. While walking along the isoheights of the slope, every sign of concentrated surface runoff is tagged in a GPS-map with no regard to the size of a specific example. When flow paths are visible through a distance of few meters, the start- and endpoint are tagged as well as a point every 2 m in between.

The purpose of this survey is to investigate spatial distribution and frequency of occurring surface runoff. Ein Samia slope contains several geological strata. Therefore it is aspired, to detect differences in surface runoff characteristics depending on ambient lithology. Since the applied method only allows for detecting flow paths on rock surfaces, the continuity of surface runoff cannot be derived from the resulting dataset.

6 Results

6.1 Infiltration characteristics and soil water balance

The distinct color change between soil sections stained with brilliant blue and those which are not, allows an accurate discrimination between these areas in the surveyed cross-sections. Water contained by stained soil sections will be referred to as 'colored water' in contrast to 'uncolored water' from soil sections which are not affected by brilliant blue.

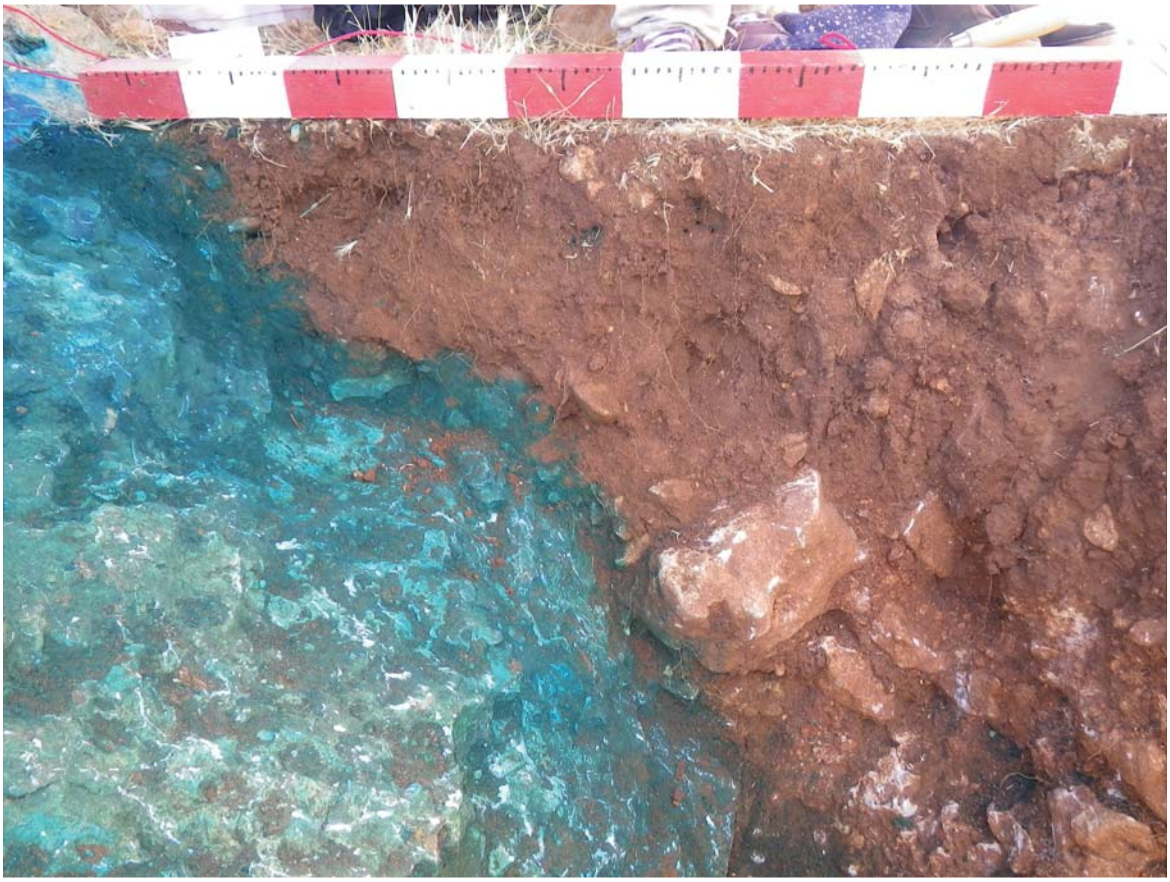

Figure 6.1: Photo of cross-section S2-5 at the coordinates N 31° 59.157, E 35° 20.604 on April 12th, 2012. Photo: Jakob Sohrt

Colored water (originating from the soil surface) shows a very different infiltration behavior than uncolored water (originating from the outcrop). While an average of 36 % of the uncolored water percolates into the fractured bedrock, 77.8 % of colored water is not accounted for in the soil water balance (see tab. 6.1). Observations of the dug cross-sections beneath the irrigated soil surface show that runoff of excess water from the outcrop surface continues below-ground. It flows along the stone-soil interface and infiltrates quickly into the widely fractured bedrock. In most cases, the flow path along the interface involves only a narrow soil column of few centimetres in height (see fig. 6.1). Since the used measurement device probes a soil cylinder of a much larger diameter, visual identification of stained flow paths could not be verified by soil moisture measurements in some cases.

No significant differences between the two experimental slopes regarding the soil water balances of surveyed cross sections have been found. Even though slightly more percolation into the bedrock is recorded in Ein Samia, the average soil water balance after the sprinkling experiment is comparable for plots in Kafr Malek and Ein Samia (see tab. 6.1).

Runoff along the interface exceeds the plot border in only 7 of 48 observed cross-sections. Lateral flow of stone-produced runoff in the soil matrix is observed in some of the cross-sections, but vertical flow and runoff on the interface dominate the flow patterns. Where infiltration from the soil surface did not proceed to the bedrock, a sharply demarked infiltration front is usually found.

The storage capacity of the soil is highly variable. An average soil column of 41.7 cm is necessary to store 50 mm of the simulated precipitation event. The minimum soil depth to fully detain the applied precipitation was found to be 16 cm.

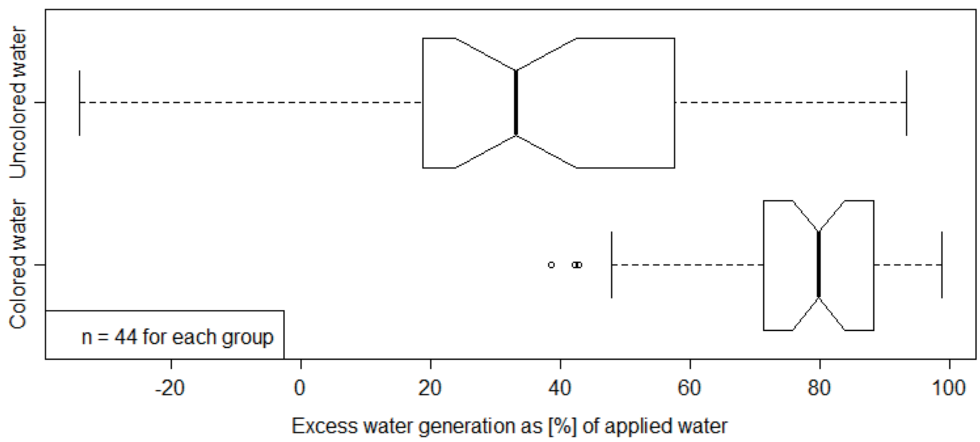

Figure 6.2: Excess water generation as [%] of applied water for stained and unstained soil sections. Calculation is carried out for every individual cross-section to take their unique geometry into account.

The occurring range of excess water generation differs significantly between the two water sources (see fig. 6.2). Excess water is defined as the deviation of the amount of water that was applied to a given plot and the soil water balance of that plot after the sprinkling experiment. While the outcrop runoff generates excess water between 38 % and 98 % of the applied amount of water, between - 34 % and 93 % of the water applied to the soil surface percolated into the bedrock. In the case of water infiltrating from the soil surface, a negative water balance is observed three times. This is the case if the actual soil moisture after the experiment was found to be lower than the assumed antecedent soil moisture.

A figure of the spatially resolved soil water balance is shown in fig. 6.3. The lower box shows a 2D interpolation of soil moisture values that were measured. The shaded area depicts the area of the cross-section which was identified as stained with brilliant blue FCF. The upper graph shows both the modelled and measured return quote of the applied precipitation water along the x-axis of the cross-section.

6.2 Model of excess water generation depending on spatial parameters

The amount of excess water generated on the experimental sites is modelled along an axis perpendicular to the extension of the interface at surface level. It was originally intended to develop separate models for water originating from the soil surface on the one hand, and water originating from the outcrop surface on the other, i.e. colored and uncolored water. However, a correlation between the distribution of colored water and spatial parameters of the respective cross-section has not been found. The developed model treats both origins of soil water alike.

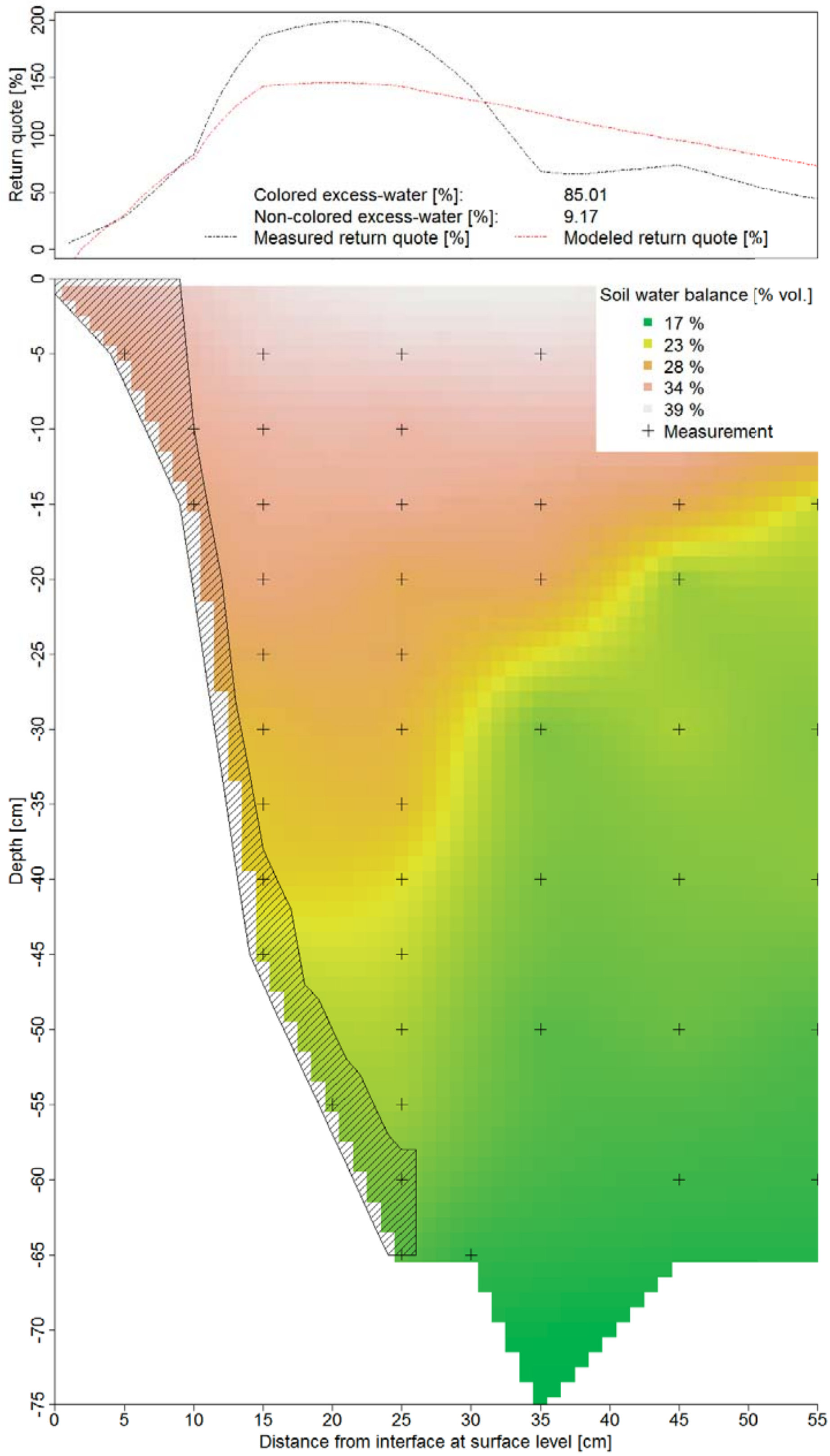

Figure 6.3: Infiltration patters along a vertical soil profile (K3-2) with display of measured and modeled values of the soil water balance along the x-axis. Both graphs share the same x-axis

Table 6.1: Excess water generation at the experimental plots after the simulated 50 mm precipitation event. Values in mm are corresponding to the total plot area of 1 m^2. Values in % correspond to the excess-water fraction of the respective water sources (colored / not colored).

Plot section	Colored excess[mm]	Uncolored excess [mm]	Colored excess[%]	Uncolored excess [%]
S1-1	22.28	14.45	74.27	72.25
S1-2	29.28	7.94	83.65	52.91
S1-3	22.85	12.97	70.31	74.10
S1-4	24.32	16.58	81.06	82.91
S1-5	9.57	17.21	47.83	57.38
S2-1	22.37	5.12	74.58	25.62
S2-3	20.93	4.85	69.77	24.27
S2-4	20.74	6.27	69.13	31.33
S2-5	20.02	8.62	66.74	43.11
S3-1	18.92	3.67	75.70	14.70
S3-2	19.52	2.34	78.09	9.37
S3-3	21.06	7.78	84.23	31.12
S3-4	19.68	1.53	78.74	6.13
S3-5	10.73	3.70	42.94	14.79
S4-1	1.86	19.80	74.31	41.69
S4-2	10.48	5.93	52.39	19.78
S4-3	12.05	11.16	57.38	38.47
S4-4	16.66	10.73	66.65	42.91
S4-5	20.45	12.09	81.80	48.34
S5-1	34.60	9.75	98.86	64.99
S5-2	30.58	6.43	94.08	36.74
S5-4	23.44	6.62	85.24	29.43
K1-1	19.67	-3.00	98.37	-10.00
K1-2	28.71	3.30	88.34	18.86
K1-3	25.80	-7.70	93.81	-34.23
K1-5	26.26	17.26	95.50	76.72
K2-1	28.24	8.53	94.12	42.65
K2-2	7.40	18.84	42.30	57.96
K2-3	2.90	14.89	38.71	35.04
K2-4	10.87	6.61	72.43	18.88
K2-5	19.15	9.49	76.58	37.95
K3-1	24.15	-6.28	96.59	-25.11
K3-2	19.13	2.52	85.01	9.17
K3-3	19.18	3.83	85.25	13.93
K4-1	17.00	8.66	97.16	26.65
K4-2	18.89	3.55	89.94	12.23
K4-3	16.82	7.07	74.75	25.71
K4-4	11.53	8.34	76.86	23.84
K4-5	21.76	6.11	72.52	30.54
K5-1	21.09	22.46	93.74	81.66
K5-2	17.70	22.66	88.49	75.54
K5-3	19.54	18.30	86.86	66.55
K5-4	16.57	21.21	82.85	70.69
K5-5	19.65	25.69	87.34	93.44

The most suitable equation to describe the return quote for any given combination of soil depth and reach along the X-axis of the cross-sections used for calibration was found to be:

$$y = (x_1 \cdot b_1 + z_1) + (b_2 \cdot x_2^{z_2}) + (b_3 \cdot x_3^{z_3}) \tag{6.1}$$

Empirical equation for calculation of return quote of infiltrated water along an axis perpendicular to the interface in [%] with:

Physical parameters:
x = distance from interface x soil depth [cm^2]; x_2 = distance from interface [cm]; x_3 = soil depth [cm]

Empirical parameters:
b_1 = -0.0467177; b_2 = 0.1452451; b_3 = 45.52499; z_1 = -59.97635; z_2 = 1.355891; z_3 = 0.4235771

The first term of eq. 6.1 ($x_1 \cdot b_1 + z_1$) is meant to predict the integral of the cross-section from the boundary point of soil and rock at surface level up to the point x_2. Even though the actual integral of any share of a cross-section can be calculated with high accuracy, the high-resolution depth profile which is necessary for this calculation is not available in the dataset of the soil depth transects. Therefore, an empirical approach for the estimation of the cross-section area is chosen. The first term of eq. 6.1 predicts the area of surveyed cross-sections up to an arbitrary value of x_2 with high accuracy. The comparison of area calculation derived from high-resolution depth profiles with alternative values from the first term of eq. 6.1 results in a Nash-Sutcliff-Efficiency of a 0.97. A total of 1441 measured values were used to calibrate this part of the model, the remaining 805 values were used for verification.

The second term of eq. 6.1 ($b_2 \cdot x_2^{z_2}$) describes the inhomogeneous soil water distribution along the x-axis of a cross-section. Since it is mostly observed that preferential flow on the rock-soil interface is not durable due to quick infiltration into the fractured bedrock it can be assumed that a surplus of soil water originating from the rock surface will rather be associated with smaller x-coordinates.

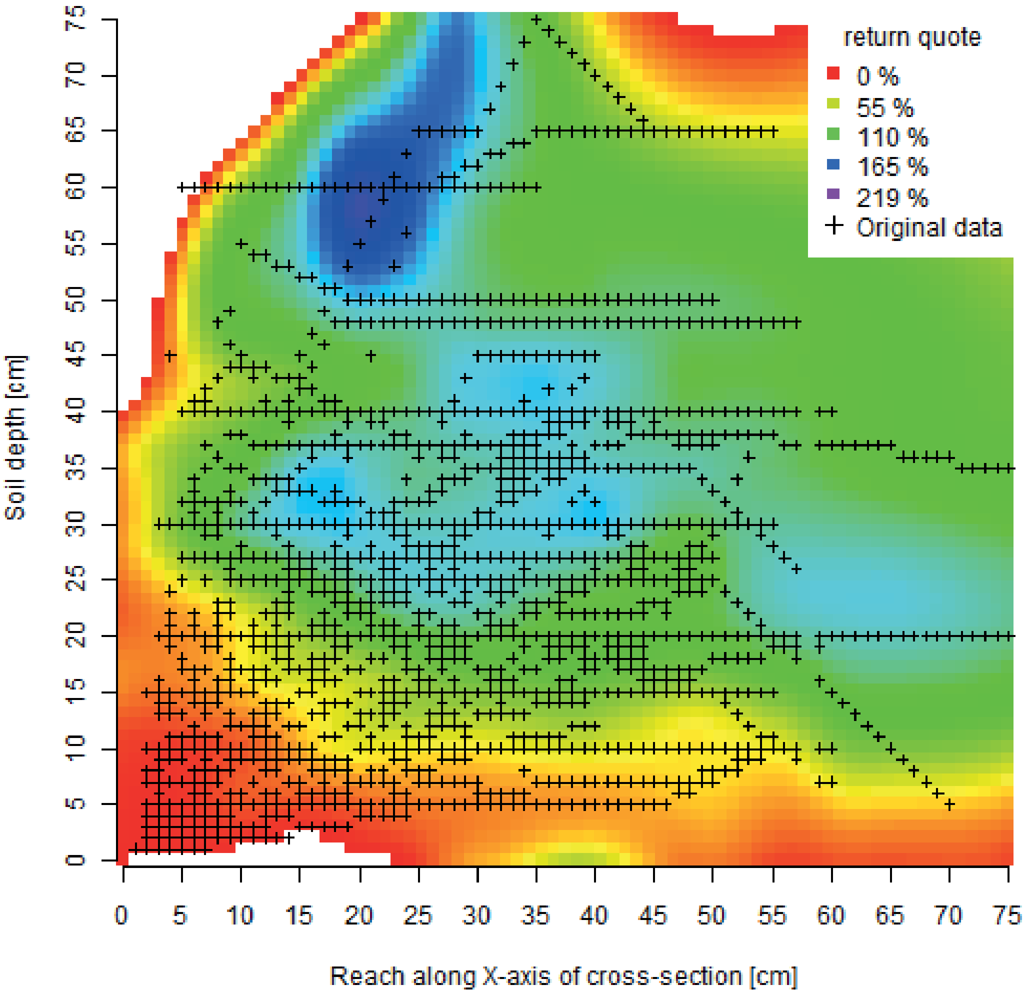

Figure 6.4: Display of the development of the return quote of applied water obtained from interpolated measurements. The whole range of encountered combinations of soil depth and distance from the interface at surface level is on display. The interpolation method in combination with sparse data and uncertain values for antecedent soil moisture caused high negative values in the upper left corner ($X_{1:20}$, $Y_{40:75}$), which are not displayed.

The third term of eq. 6.1 ($b_3 \cdot x_3^{z_3}$) is meant to take into account that the return quote of precipitation water in the soil[%] for a given x-coordinate highly depends on the available storage capacity in the soil. In this simplified approach, storage capacity of the soil is assumed to be predominantly determined by soil depth.

The complete equation is fitted to 1441 points of measured data and verified on the remaining 805. A Nash-Sutcliffe-Efficiency of 0.7 is found for the comparison of calculated and measured values, even though it is obvious, that eq. 6.1 cannot reproduce the complex topography representing the distribution of the variable 'return quote' as displayed in fig. 6.4.

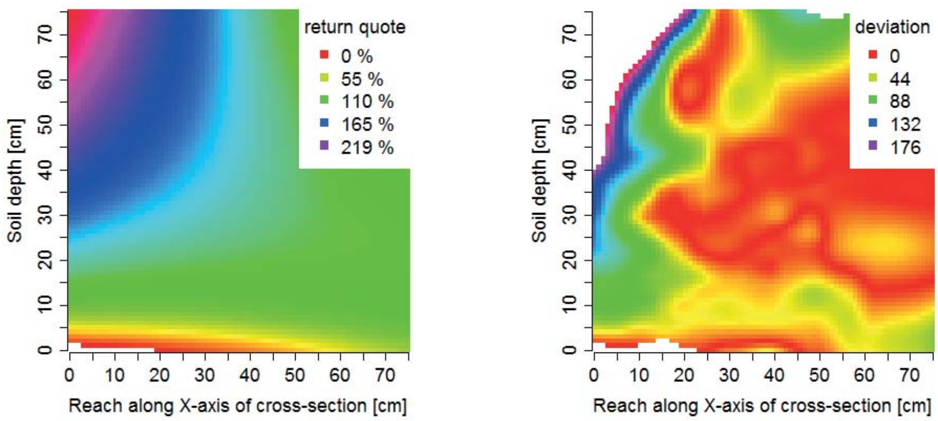

Figure 6.5: Model results and comparison to original data. The left plot depicts values of eq. 6.1 for all encountered combinations of soil depth and reach along the X-axis of a cross section. The right plot shows the deviation between the model results and interpolated average values of the soil moisture measurements.

The return quote [%] predicted by eq. 6.1 generally increases with both soil depth and perpendicular distance from the interface at surface level (see fig. 6.5). However, if the distance from the interface exceeds ∼40 cm the predicted return quote ceases to increase.

The prediction error is generally higher for larger values of both parameters but does not show a distinct type of dependence. Still, it is highest for a soil depth $\succ$ 40 cm and at distance from the interface $\prec$ 20 cm.

6.3 Estimating infiltration in soil not influenced by a soil-rock interface

To compensate for the lack of control experiments in pure soil distant from rock outcrops, shares of existing cross-sections are selected where no interface-induced effects are observed. This applies for sections on the edge of the plots opposite from the interface and shallow soil sections which can not fully retain the applied precipitation. A linear model is found to be the most suitable equation to calculate the return quote of incoming precipitation in pure soil. This equation is only applicable for the measured range of antecedent soil moisture. The equation is fitted with return quote as dependent and soil depth as independent variable (see fig. 6.2). The equation is fitted to 400 data values and reaches a adjusted R^2 of 0.79

$$y = 2.398 \cdot x \tag{6.2}$$

Empirical equation for the prediction of the return quote in pure soil with: x = soil depth [cm]; y = return quote of applied water [%]

Due to the fact that the estimation of antecedent soil moisture is most likely associated with a large prediction error, return quotes $\succ$100 % are a common occurrence, even when no preferential flow patterns are visible. The large prediction error is also indicated by the fact that a large margin in the values (of return quote) for a single location with identical depth values can be found. At the same time, the return quote often falls below the applied amount of water even in thick soils layers with fairly homogeneous flow patterns and a sharply demarked infiltration front.

6.4 Antecedent soil moisture

In almost all cases, soil moisture increases along the depth profile with a strong linear trend. Still a large range of values occurs within repeated measurements in the same depth of a respective plot (see fig. 6.6). The average variation of measured values for one location is generally higher than the variation of average measured values between different locations. No significant difference between average antecedent soil moisture measurements for given depth classes on the two experimental slopes was found.

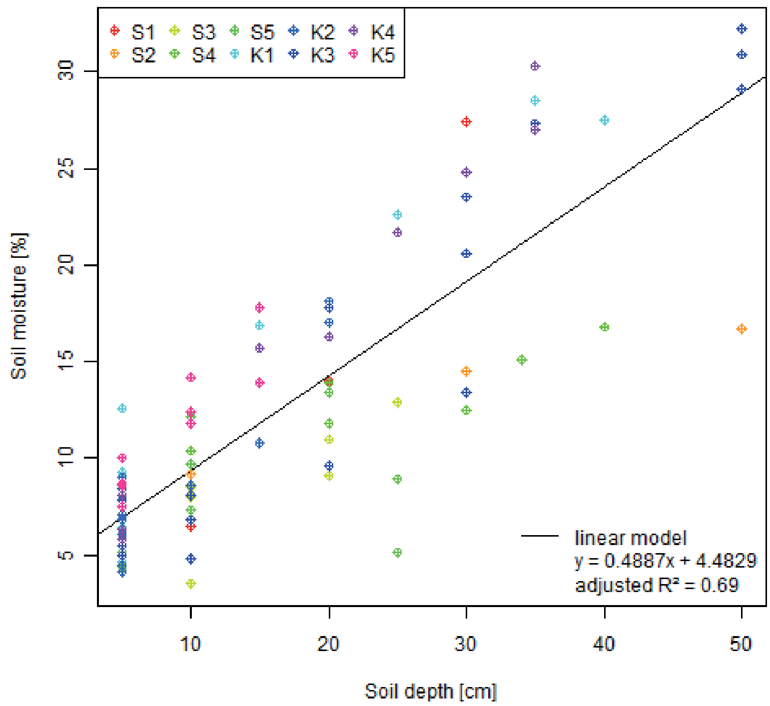

Figure 6.6: Display of all measured values of antecedent soil moisture and a linear model for all data points.

6.5 Below ground flow velocity

Three probes (Decagon 5MTE/M©) are positioned directly at the soil-rock interface in depths of 10, 30, and 40 cm. The two remaining probes are positioned in a horizontal distance of 35 cm to the interface at surface level in depths of 10 and 30 cm, respectively. A desiccation crack is found discontinuously along the rock-soil interface. The infiltration front did not reach the probe at depth of 30 cm in the soil matrix by the time the measurement

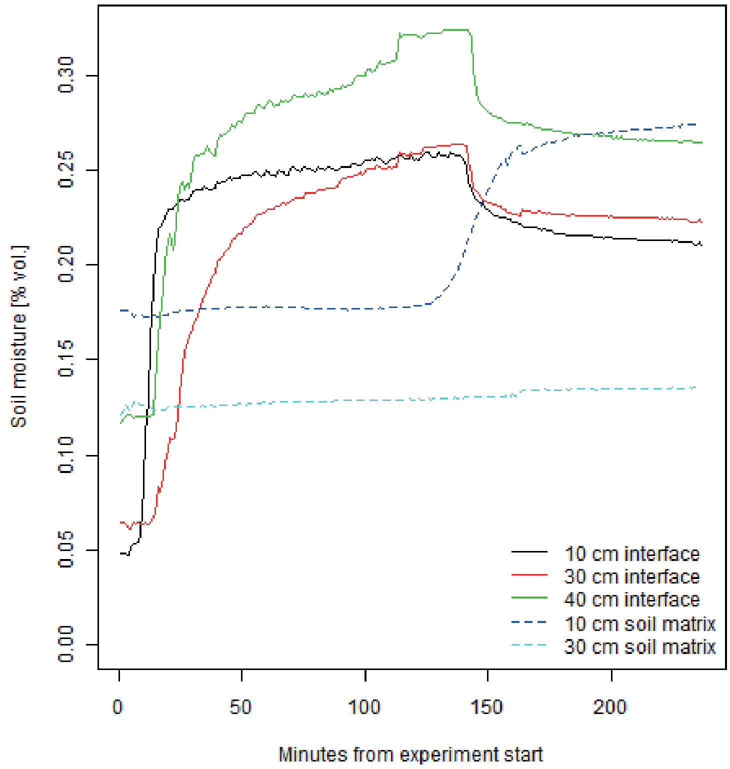

Figure 6.7: Time series of soil moisture measurements at five points in cross-section K3-1.

was aborted after a runtime of 18 hours. Infiltration along the interface takes place at a much higher speed and reaches higher depths compared to infiltration in the soil matrix (see fig. 6.7). The infiltration front reaches the probes along the interface 10, 13, and 15 minutes respectively after the start of the sprinkling experiment whereas it takes 125 minutes until it reaches the upper probe in the soil matrix. This results in a vertical flow velocity of 2.8 $\mathrm{cm\,min^{-1}}$ along the interface and 0.08 $\mathrm{cm\,min^{-1}}$ in the soil matrix. The increase of soil moisture after the initial rise occurs much faster at the probes along the interface than at the probe in the soil matrix. Hanf (2010) found values of saturated conductivity to be in a range of 0.7 to 2.28 $\mathrm{cm\,min^{-1}}$ for the nearby Ein Samia hillslope with an average value of 1.24 $\mathrm{cm\,min^{-1}}$.

The infiltration rate along the interface can be estimated as well by comparing the contributing area on the outcrop surface and the (stained) infiltration area. The outcrop runoff infiltrates within an average distance of 10.04 cm of the interface at surface level. Given that an average of 50 cm of outcrop contributes to the runoff infiltrating here, this results in an average infiltration rate of 0.17 $\mathrm{cm\,min^{-1}1}$ for the simulated rainfall intensity of 20.61 $\mathrm{mm\,h^{-1}}$.

6.6 Estimation of excess water generation along the soil depth transects

Under consideration of eq. 2 it is assumed that for locations with a soil depth $\succ$ 41.7 cm (= 100 = 2.398x see 6.2) no excess water is produced after a 50 mm precipitation event assuming a antecedent soil moisture profile according to eq. 6.2. In order to calculate the excess water generation along the soil depth transects the following assumptions are made:

- Stone surfaces produce 100 % excess water. While this is not true in reality the water fraction from the stone surface that gets retained in the soil matrix is accounted for in eq. 6.1.

- Deep soil (soil depth $\succeq$ 41.7 cm) in a distance of at least 50 cm from the next rock outcrop produces 0 % excess water.

- Shallow soil (soil depth $\prec$ 41.7 cm) in a distance of at least 50 cm from the next rock outcrop produces excess water according to eq. 6.2.

- Soil sections influenced by a rock-soil interface produce excess water according to eq. 6.1.

The results of the calculations based on the previously stated assumptions are presented in tab. 6.2.

An average of 86 % of the surveyed area contributes to infiltration of water below the soil layer (see tab. 6.2). The magnitude of the contribution varies strongly between different surface types. Stone surfaces have a share of 31 % of the surveyed area while generating 62 % of the water that percolates below the soi layer. Shallow soils account for 28 % of the area and 27 % of the total excess water. Infiltration from the soil surface in areas neighbouring the rock-soil interface accounts for the remaining 10 %. The average amount of water percolating below the soil layer is 26 mm in Ein Samia and 22 mm in Kafr Malek. This accounts for 52 % respectively 45 % of the hypothetical 50 mm precipitation event.

Table 6.2: Characteristic values of surface type composition and excess water generation for a hypothetical 50 mm precipitation event from the surveyed transects in Ein Samia and Kafr Malek

	S1	S2	S3	S4	K1	K2	K3	Average
Soil $\prec$ 50 cm to interface [%]	32.68	22.55	33.99	29.41	16.3	20.59	18.3	24.83
Deep soil area [%]	12.75	11.96	0.2	12.75	35.42	12.75	9.8	13.66
Shallow soil area [%]	21.9	28.24	9.68	38.24	21.94	50.98	28.76	28.53
Stone area [%]	23.86	35.49	55.53	19.61	24.76	15.69	43.14	31.15
NA area [%]	8.82	1.76	0.59	0	1.57	0	0	1.82
Interface excess [%]	9.31	12.83	18.43	12.62	1.21	8.64	4.42	9.64
Deep soil excess [%]	0	0	0	0	0	0	0	0
Shallow soil excess [%]	20.24	24.23	34.22	21.87	23.13	24.06	24.15	24.56
Stone excess [%]	100	100	100	100	100	100	100	100
Interface excess [mm]	3.01	2.79	5.39	3.71	0.2	1.78	0.81	2.53
Deep soil excess [mm]	0	0	0	0	0	0	0	0
Shallow soil [mm]	4.43	6.84	3.31	8.36	5.07	12.27	6.95	6.75
Stone excess [mm]	11.93	17.75	27.77	9.8	12.38	7.84	21.57	15.58
Total excess [mm]	19.37	27.38	36.47	21.87	17.65	21.89	29.33	24.86

6.7 Particle size and soil organic carbon content

No significant discrepancy between the two groups of soil samples - close to the interface in comparison to samples obtained 50 cm away from the interface - has been found (see tab. 6.3). However, significantly higher fractions of clay are found compared to a study on the same slope in Ein Samia by Hanf (2010) who found clay fractions to be between 10 % and 25 %, while clay fractions in the samples displayed in fig. 6.8 range from 35 % to 65 %.

As for the soil organic carbon, there is no significant difference, either between the sampling locations inside the plots or between the experimental sites.

The recorded soil types of the experimental sites are Rendzina and Terra Rossa , according to Dan & Raz (1970). Samples of all experimental sites contained undissolved carbonates as proofed by the reaction with hydrochloric acid. An intense reaction was observed on every sample, each location is represented through two samples. Since Terra Rossa contains reportedly not more than traces of undissolved carbonates (Singer, 2007), the soil on all experimental plots can be assumed to be Rendzina.

The soil color is found to be homogeneous through the depth profile on all plots. Topsoil layers of pure organic genesis have not been observed. Stone content tends to be highly variable between plots and to increasing with depth and vicinity to the slope toe. . Root density in the topsoil is found to be continuously high, decreasing with depth. Tender roots

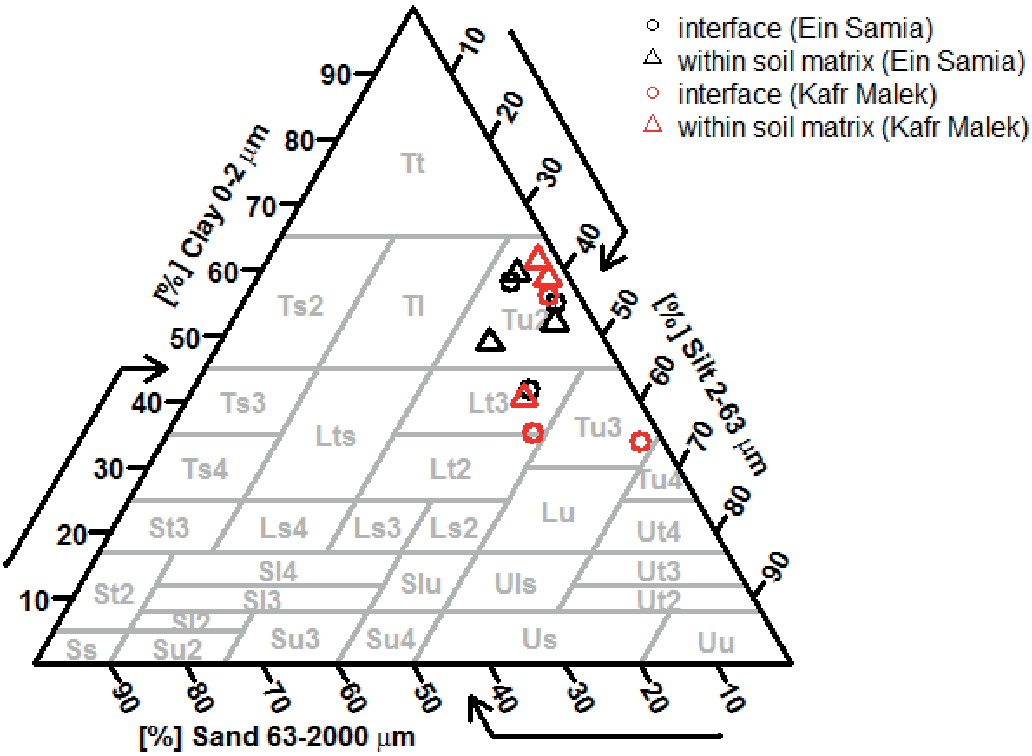

Figure 6.8: Texture triangle with the particle size distribution of probed soil samples.

Table 6.3: Texture analysis of the measured soil samples. The sample denomination implies: S = Ein Samia, K = Kafr Malek - Plot number - 1 = sample from rock-soil interface, 2= sample 50 cm away from interface, Accuracy = Accuracy of the soil particle size analysis

Sample	Soil organic carbon [%]	Clay [%] (2 μ m)	Silt [%] (63-2 μ m)	Sand [%] (2000-63 μ m)	Accuracy [%]
S-02-1	3.15	52.93	30.59	7.39	90.90
S-02-2	3.44	58.58	33.45	6.41	98.44
S-04-1	4.18	40.92	43.42	13.39	97.73
S-04-2	4.00	48.43	35.37	15.22	99.02
S-05-1	6.81	56.78	42.61	3.74	103.13
S-05-2	4.87	53.15	43.67	5.46	102.28
K-03-1	4.58	56.65	40.26	4.07	100.99
K-03-2	2.09	59.75	39.17	2.90	101.82
K-04-1	4.78	33.75	62.83	3.16	99.73
K-04-2	2.67	60.78	35.34	2.76	98.88
K-05-1	5.09	34.69	47.79	16.42	98.91
K-05-2	6.03	38.78	42.66	14.49	95.93

are found to a depth of 60 cm at least, even though soil sections with almost no roots due to soil compaction and/or high stone content are frequent. The surface of the rock-soil interface near the soil surface is usually covered with a mat of interlocked roots. The stone content is quite variable amongst the plots and generally lower in Kafr Malek. Isolated gravel and boulders are found frequently within the soil matrix. This strengthens the assumption that soils in the study areas are widely disturbed through either/both natural and human influences. Cracks in the soil - mostly vertical - are a common occurrence up to a depth of about 30 cm. There is no indication for continuous bioturbation, earthworms are only very rarely observed

6.8 Soil depth survey

The survey covers a total of 2100 points, on 1333 of which soil depth was measured. The distribution of soil depth classes shows clear differences between the two experimental sites (see 6.10). The average soil depth in Ein Samia is considerably lower than in Kafr Malek. In addition, the distribution of soil depths differs. While in Ein Samia the frequency of soil depth classes decreases logarithmically with increasing soil depth, a linear decline is present in Kafr Malek. Maximum soil depth is similar on both locations. Due to the restricted length of the probe it cannot be ruled out that deeper soils may exist on the surveyed transects. The average soil depth is not correlated with proximity to the hillslope toe/top which applies for each individual transect and average values from all cross-sections. Additionally, there is no correlation between frequency of rock outcrops and slope position. Variation in frequency of rock outcrops between different parenting materials occurs along the slope in Ein Samia. The transect S3, which is located exclusively on Amminadav-limestone, shows a relatively high fraction of rock outcrops (55 %) in comparison to the transects of S1 (30 %) and S2 (34 %). Differences in frequency of outcrops between other geological strata - provided they could be discriminated - seem to be rather marginal.

A model is developed to predict soil depth as a function of proximity to a soil-rock interface at surface level and ambient cover type. No apparent correlation between these parameters could be found, thus ruling out a further upscaling of groundwater recharge.

The survey confirms that surface cover types vary strongly between the two study sites (see fig. 6.9). Bare rock accounts for 40 % of the surface cover in Ein Samia but only 26 % in Kafr Malek. Shrubs are considerably more frequent in Kafr Malek (40 %) than in Ein Samia (16 %). Bare soil and gravel account for 16 % of the surface cover on both slopes.

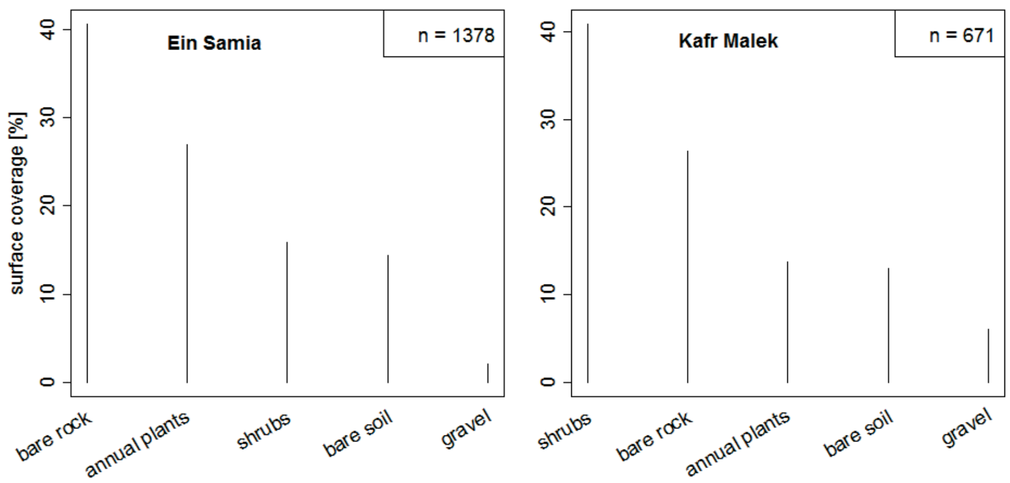

Figure 6.9: Surface cover types in Ein Samia and Kafr Malek according to the properties recorded along the soil depth transects.

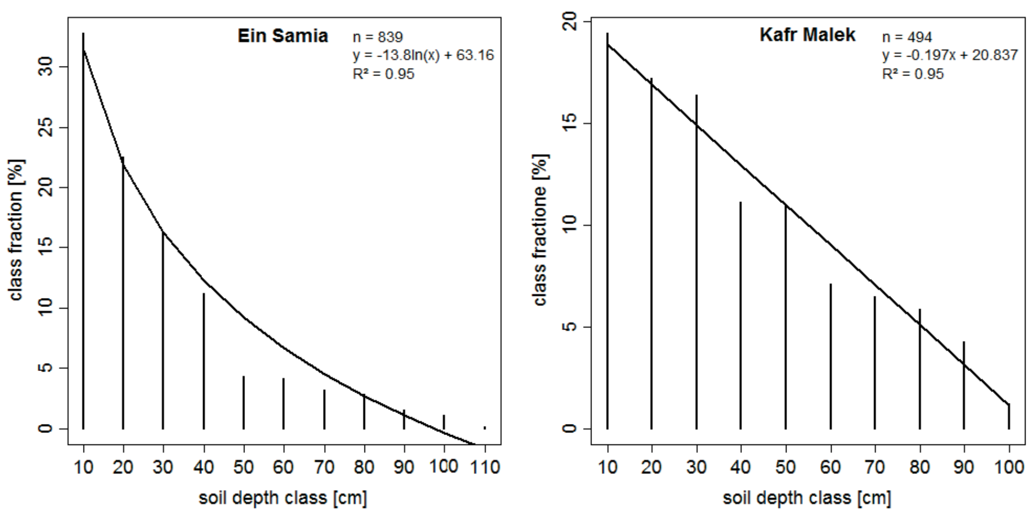

Figure 6.10: Soil depth distribution along transects in the experimental sites close to Ein Samia and Kafr Malek.

6.9 Mapping of surface runoff

Signs of runoff on stone surfaces are observed almost exclusively on the north-eastern part of the Ein Samia hillslope, which corresponds to the transition of ambient geology to Amminadav. Signs of runoff are usually recorded on large outcrops and downslope of shallow soil pockets. Still there is no apparent evidence of fluvial soil erosion, thus limiting the expected runoff quantity/intensity. Signs of surface runoff occur only sporadically on the eastern part of the slope and are limited to very flat outcrops downslope of very shallow and steep soil pockets with a favorable micro topography.

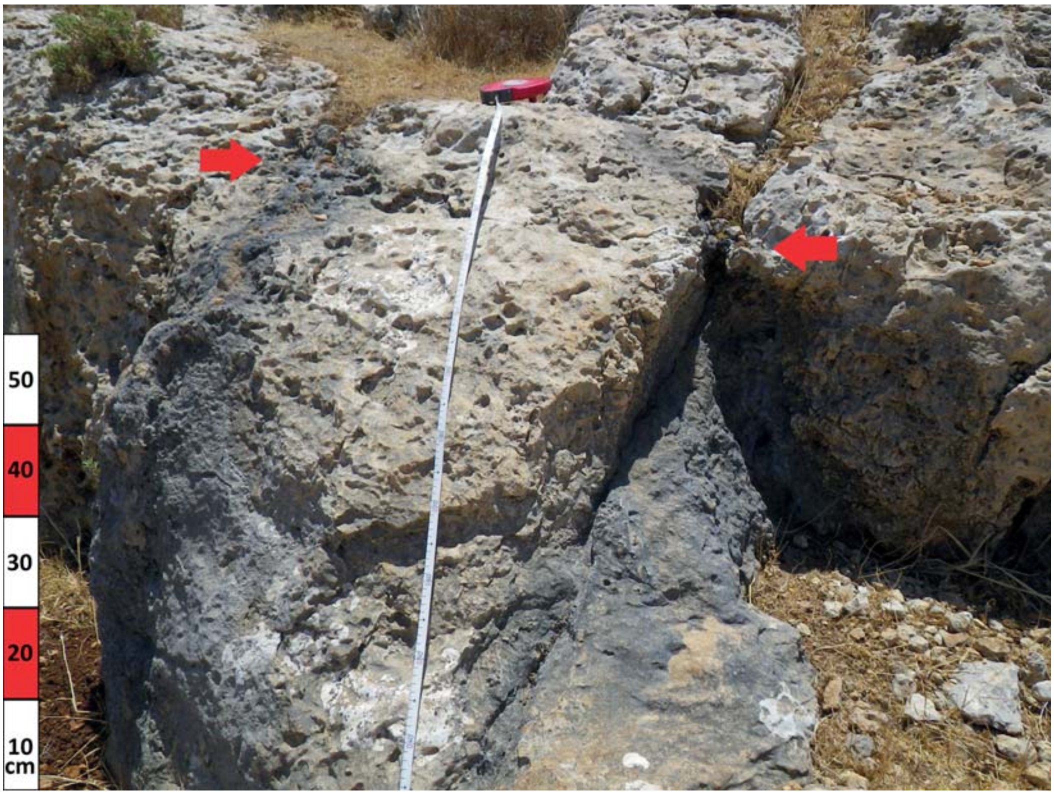

Figure 6.11: Two preferential flow paths on the surface of a rock outcrop. The upper end of the flow path is marked with a red arrow

7 Discussion

7.1 Method

The rainfall simulation equipment turns out to be suitable for the experiments carried out. Size and weight of the experimental setup allow for transport by backpack and, thus, for accessibility of remote plot locations. Pump and sprinklers are reliable even though spare nozzles should always be provided in case of a plugging. A 12 V 9 Ah battery provides sufficient power for at least three hours of operation. A more stable frame with height-adjustable legs as basis for the nozzles would be desirable.

Soil moisture measurements proved to be difficult in a lot of cases due to unfavorable soil conditions. Even though the sensing head of the UMS ML2x©-probe provides considerable stability the encountered soils proved to be too tightly arranged in some cases to allow for spatially dense measurements. Soil moisture measurements are restricted as well by high stone/gravel content since a stone-free soil cylinder of 3 cm width and 6 cm length is needed for measurements with the UMS ML2x©-probe. Perhaps a smaller sensing head would be more adequate for soil moisture measurements under the encountered conditions.

The existence of preferential flow along the soil-rock interface is sufficiently confirmed by the dimension of stained flow paths in consideration of the applied precipitation intensity. Still, it would be favorable to confirm these findings with more time series of soil moisture measurements during and after the sprinkling experiments.

7.2 Antecedent Soil moisture

The dataset for antecedent soil moisture can be assumed to be the largest single source of uncertainty in the water balance for a respective cross-section/plot. Since there is no non-destructive way to do so this parameter could not be measured directly on the experimental plots. Even though antecedent soil moisture was measured at the closest possible location from the respective plot the spatial transfer of this parameter is most likely associated with an error. The same goes for the presetting that antecedent soil moisture is horizontally homogeneous, which was assumed for each cross-section. This might not be a problem regarding the water balance of a complete cross-section; however, it certainly is problematic with respect to individual points within a cross-section. Since spatial variation of soil moisture is the core matter of interest of this thesis the absence of precise knowledge about spatial distribution of antecedent soil moisture can be considered a serious knowledge gap. There is no apparent solution to this problem, it would, however, be desirable to at least quantify the variability of antecedent soil moisture in high resolution in order to determine the possible range of the resulting water balance error.

7.3 Soil Water Balance

Spatial proximity to the rock-soil interface seems to promote infiltration into deeper soil layers. This applies to infiltration from the soil surface as well as to runoff from the rock-outcrop as it can be observed in most of the spatially resolved soil water balances (see Appendix). The explanation for the former case could be that the soil layer directly above the interface gets temporarily saturated by runoff from the outcrop. When water from the soil surface percolates to this depth it cannot infiltrate vertically anymore and flows laterally on the soil layer, which is saturated by the water originating from the outcrop-runoff. This would be a self-energizing effect since the saturated layer gets constantly thickened, which leads to water from upper soil layers to participate in the saturated flow, causing it to ultimately infiltrate more deeply. The existence of temporarily saturated conditions on the interface is confirmed by the results of the flow velocity experiment (see fig. 6.7) where the flow velocity along the interface exceeds by far the possible speed of unsaturated matrix flow and lays above the range of measurements for saturated conductivity on the nearby slope in Ein Samia (Hanf, 2010).

The fact that infiltration in the soil matrix was found to be almost exclusively vertical and no surface runoff or ponding was observed regardless of vegetation type shows that the controlling factors for infiltration on the experimental slopes are fundamentally different from the findings of Abrahams & Parsons (1991) in Arizona and Bergkamp (1998) in Spain, where vegetation cover was of major importance for infiltration patterns. The importance of vegetation on infiltration rates arises from the protection from surface sealing, preferential flow paths along root channels, and enlargement of cracks in the bedrock by root growth. Such effects are not observed in the course of the conducted experiments. The infiltration capacity of the soils encountered in the experiments always exceeds the applied precipitation intensity of 20.6 $\mathrm{mm\,h^{-1}}$.

The high infiltration capacity of the soil and the fractured bedrock material on the experimental slopes may be described as crucial for the observed properties of percolation below the soil layer. Relatively impermeable bedrock (Lange et al., 2003) and soil surface crusting (Yair, 1983) can lead to large-scale lateral displacement of water. Since the observed recharge mechanism relies on preferential flow paths with a strong vertical component, lateral displacement will result in additional soil water storage and, thus, less recharge.

The small plot size results in a knowledge gap regarding the generation of runoff from outcrops larger than 1 m in diameter. Outcrops extending over several meters are recorded in the soil depth survey; additionally, channelling on the rock surface leads to concentration of outcrop runoff. This could lead locally to the transgression of soil infiltration capacity, resulting in surface runoff exceeding the outcrop surface. Furthermore, it remains to be investigated if the percolation rate into the bedrock remains stable over the course of multiple consecutive rainfall events. It has to be taken into account that bottlenecks could exist in the vertical profile of the permeable bedrock sections, which would temporarily decrease the infiltration capacity.

Even though the conducted experiments enable to study both undisturbed infiltration in the soil matrix and infiltration influenced by the interface it would be desirable to study the infiltration response on pure soil plots further away from a soil-rock interface. Such control experiments would increase the validity of the conducted experiments.

7.4 Transferability of model results

The spatial transferability of the model can be expected to be limited. The results of the soil depth survey indicate that controlling factors for the proposed regional recharge mechanism are spatially highly variable. Therefore, it cannot be assumed that the results of the regional recharge calculations are directly applicable to surrounding areas. Outcrop frequency and extent can be derived from high-resolution aerial photographs. However, as long as influencing factors for soil depth distribution are not isolated there is still the need for local soil depth determination in order to apply the developed recharge approach.

The main confinement regarding the temporal transferability of the developed model is the fact that all conducted sprinkling experiments simulate a uniform precipitation event of 50 mm over the course of 146 minutes. Thereby, the parameterization of eq. 6.1 is only applicable to precipitation events with these characteristics. Even though this was clear before the start of the experiments the results confirm the initial assumption that repetitive experiments under uniform conditions are necessary to cover the large variability of ambient conditions. Additionally, the model parameterization is bound to the ambient soil moisture measured during the sprinkling experiments. The soil moisture profile under semi-arid conditions with one distinct raining season can be expected to follow a seasonal cycle. Assuming that the average soil moisture will be much lower at the beginning and much higher during the raining season there might be a considerable range of deep percolation following a 50 mm precipitation event depending on the antecedent soil moisture.

Thus, the outcome of this thesis does not empower to predict groundwater recharge from real precipitation data. It does, however, serve as a hint on how different surface types, the soil-rock interface, and soil depth contribute to infiltration below the soil layer after an exemplary precipitation event.

7.5 Infiltration rates and preferential flow

The results of the experiment on below-ground flow velocity are difficult to interpret. The time lag between the start of the sprinkling experiment and the first increasing values from the reading of the probes implies a hydraulic conductivity that lies above the range obtained by Hanf (2010). While the reading of the probe on the soil matrix could be somehow compatible with the findings of Hanf (2010), the readings along the soil-rock interface are certainly not. This could be blamed on the disturbance to the plot caused by the need to dig a cross-section before the experiment to install the probes.

The estimation of infiltration rates at the interface derived from the extent of stained flow paths, however, confirms that infiltration rates at the interface exceed by far the saturated conductivity in the soil matrix. This is a strong indication of the existence of preferential flow paths along the interface. This is supported by the fact that the readings from the probes at the interface show a sharply demarked infiltration front while it takes much longer for the surveyed point in the soil matrix to reach peak soil moisture.

However, the flow rates derived from the assessment of the stained flow paths are still one magnitude order smaller than those measured in the soil moisture time series.

A difference between these two methods should be expected since the geometry of a stained flow path represents its maximum extent, which could be enlarged by diffusion of stained water over the course of the experiment. The time lag between the start of precipitation and increasing soil moisture in a given depth corresponds to the minimum amount of time water needs to infiltrate into that depth. Desiccation cracks and the general swelling of the soil during the experiment can be expected to lower the infiltration rate over time, indicating that the time lag measurement might overestimate the average infiltration capacity.

Even though the mentioned limitations do not allow a detailed assessment of infiltration rates at the soil-rock interface it can be concluded that the infiltration capacity lays between 0.17 and 2.8 $\mathrm{cm\,min^{-1}}$, which is far above the hydraulic conductivity for ambient soil as described by Hanf (2010). Therefore, it must be assumed that preferential flow takes place along the soil-rock interface.

7.6 Particle size analysis and organic carbon content

The result of the analysis can be assumed to be accurate since the individual particle size classes add up very close to 100 % except in one case (see tab. 6.3). Still, the small number of samples makes it appear doubtful that the results are representative for the study areas. Hanf (2010) found considerable differences in clay content on the Ein Samia slope even within the same profile, also trends in particle size distribution were not bound to increasing sample depth. Additionally the samples by Hanf (2010) show considerably lower clay content than the samples analyzed in this study. This suggests that particle size distribution in ambient soils is variable to some extent while the controlling factors are not clear. However, the hypothesis that clay and soil organic carbon content increases with proximity to the soil-rock interface cannot be confirmed by the results of this study.

7.7 Soil depth distribution

Soil depth distribution is found to be spatially highly variable with shallow profiles outnumbering deep ones. Influencing factors for the recorded distribution are hard to determine. Protruding outcrops can be assumed to be barren because of lacking possibilities for soil accumulation. The variation of soil depth over short distances in smoother areas of the slopes points towards the occurrence of soil displacement. Since the soil depth survey does not show a decline in average soil depth towards the hilltop it can be assumed that fluvial erosion is of minor importance at the study sites. This does not exclude the possibility of aeolian erosion and sedimentation, which would be more dependent on wind exposure than just elevation.

7.8 Mapping of surface runoff

The findings of the survey show that lateral displacement of incoming precipitation does occur on the experimental slope of Ein Samia under favorable conditions, depending mainly on geology. This confirms the assumption that the permeability of the ambient bedrock is of high importance for net vertical infiltration. The strong dependence of surface runoff to ambient geology also highlights the fact that the developed model is only applicable under the local conditions.

8 Conclusion

The applied approach successfully reveals direct groundwater recharge mechanisms on the slopes in the study area. Percolation into the bedrock at the surveyed locations is found to be highly dependent on the presence of rock outcrops as rainwater redistribution areas. This offers new possibilities for spatially resolved process-based modelling of groundwater recharge in the area since the distribution of rock outcrops is easily available from aerial photographs. The second controlling parameter for local groundwater recharge, soil depth, cannot be obtained through remote sensing right now. This could be substituted by a statistical approach using average soil depth distribution rather than actual spatial soil depth data. Until controlling factors for local soil depth distribution are found this still requires local investigations.

Still, the established hypothesis needs to be tested on a broader basis including the effect of various states of antecedent soil moisture, soil type, and bedrock to be applicable to actual precipitation time series. Findings of Lange (2003) and Yair (1983) also indicate that the observed percolation properties may only be applicable locally since the cited studies indicate a much lower permeability of present bedrock material both north and south of the experimental sites of this thesis. This could very well be due to the difference in geology but remains to be investigated properly.

Depending on the current state of soil moisture it is entirely possible that infiltration through the soil matrix contributes a considerable share to groundwater recharge during the wet season.

Nevertheless, as long as the infiltration capacity of soil and bedrock are not exceeded, hillslopes in the study area with frequent rock-outcrops can be assumed to be important for the local groundwater recharge.

9 Declaration of Originality

I hereby declare that the work in this thesis is completely my own. To the best of my knowledge, the used methods have been declared accurately. Only the denoted means have been used and all references have been clearly cited according to scientific standards.

The content of this thesis has not been submitted in this or similar form for publication before.

The original measurement data this thesis is based on as well as the code that was used to process it can be received from the appendix-CD or directly from the author.

Place, Date: ______________________________

Signature: ________________________________

Contact: jakob.sohrt@gmx.de

10 Acknowledgement

The development of this thesis was made possible because of several people who helped and supported me during the process. I would like to thank these people and acknowledge their efforts:

PD Dr. Jens Lange and Dr. Heike Puhlmann will review and grade this thesis and have provided inspiration and constructive criticism. PD Dr. Jens Lange also participated greatly in the development of the hypothesis tested in this study. Fabian Ries greatly supported the fieldwork and shared infrastructure and meteorological data. Dr. Helmer Schack-Kirchner kindly allowed me to use the laboratory of the Institute of Soil Science and Forest Nutrition. My work there was supported and instructed by Petra Großmann and Petra Wiedemer. Proofreading was carried out by Lukas Macher.

The contact to and communication with the local population at the experimental sites was greatly assisted by Awad Mohammad Rashid Hamayil, which allowed for a continuous and undisturbed experimental process.

Bibliography

DIN 4022: Benennen und Beschreiben von Boden und Fels. 1987.

Study of the eastern aquifer and master plan for bulk water supply systems in the southern west bank. Technical report, House of Water and Environment. Ramallah-Al Bireh, Palestine, 2010.

Arthol D. Abrahams and Anthony J. Parsons. Relation between infiltration and stone cover on a semiarid hillslope, southern arizona. *Journal of Hydrology*, 1991.

A. Ayalon, M. Bar-Matthews, and E. Sass. Rainfall-recharge relationships within a karstic terrain in the eastern mediterranean semi-arid region, israel: delta18o and deltad characteristics. *Journal of Hydrology*, 1998.

Z. B. Begin. The geology of the jericho sheet (geological map series 1:50 000). *Bulletin of the Geological Survey of Israel*, 1974.

G. Bergkamp. A hierarchical view of the interactions of runoff and infiltration with vegetation and microtopography in semiarid shrublands. *Catena*, 1998.

Beuth. *DIN ISO 1127: Bestimmung der Partikelgröenverteilung in Mineralböden*. 2002.

Hans-Peter Blume, Gerhard W. Brümmer, Rainer Horn, Ellen Kandeler, Ingrid Kögel-Knabner, Ruben Kretzschmar, Karl Stahr, Berndt-Michael Wilke, Sören Thiele-Bruhn, and Gerhard Welp. *Scheffer / Schachtschabel: Lehrbuch der Bodenkunde*. Springer Heidelberg, 2010.

N. Bockgard and A. Niemi. Role of rock heterogeneity on lateral diversion of water flow at the soil-rock interface. *Vadose Zone Journal*, 2004.

A. Cerd‘a. Relationships between climate and soil hydrological and erosional characteristics along climatic gradients in mediterranean limestone areas. *Geomorphology*, 1998.

J. E. Christiansen. Irrigation by sprinkling. *California Agricultural Experiment Station Bulletin*, 1942.

T. Cooley. Geological and geotechnical context of cover collapse and subsidence in mid-continent us clay-mantled karst. *Environmental Geology*, 2002.

J. Dan and Z. Raz. *Soil association map of Israel. 1:250 000.* Ministry of Agriculture. Agricultural research Organization and Soil Conservation and Drainage Department. Survey of Israel, 1970.

P. J. Diggle and P. J. Ribeiro. *Model Based Geostatistics.* Springer, 2007.

J. W. Finch. Estimating direct groundwater recharge using a simple water balance model - sensitivity to land surface parameters. *Journal of Hydrology*, 1998.

J. Freer, J. J. McDonnell, K. J. Beven, N. E. Peters, D. A. Burns, R. P. Hooper, B. Aulenbach, and C. Kendall. The role of bedrock topography on subsurface storm flow. *Water Resources Research*, 2002.

Judit German-Heins and Markus Flury. Sorption of brilliant blue fcf in soils as affected by ph and ionic strength. *Geoderma*, 2000.

B. Gjettermann, K. L. Nielsen, C. T. Petersen, H. E. Jensen, and S. Hansen. Preferential flow in sandy loam soils as affected by irrigation intensity. *Soil Technology*, 1997.

Andrea Hanf. Estimation of groundwater recharge by modeling of oil moisture movement in a semiarid catchment, wadi auja, west bank. Master's thesis, 2010.

A. Horowitz. *The Quaternary of Israel.* Academic Press, New York, London., 1979.

Heinz Hötzl. Groundwater recharge in an arid karst area (saudi arabia). *Application of Tracers in Arid Zone Hydrology (Proceedings of the Vienna Symposium, August 1994)*, 1995.

J. Lange, N. Greenbaum, S. Husary, M. Ghanem, C. Leibundgut, and A. P. Schick. Runoff generation from successive simulated rainfalls on a rocky, semi-arid, mediterranean hillslope. *Hydrological Processes*, 2003.

Christian Leduc, John Bromley, and Pierre Schroeter. Water table fluctuation and recharge in semi-arid climate: some results of the hapex-sahel hydrodynamic survey (niger). *Journal of Hydrology*, 1997.

David N. Lerner. *Geochemical Processes, Weathering and Groundwater Recharge in Catchments*. A. A. Balkema, 1997.

J. J. McDonnell. The influence of macropores on debris flow initiation. *Quarterly Journal of Engineering Geology*, 1990.

Daniel R. Muhs, James Budahn, Anna Avila, Gary Skipp, Joshua Freeman, and DeAnna Patterson. The role of african dust in the formation of quaternary soils on mallorca, spain and implications for the genesis of red mediterranean soils. *Quaternary Science Reviews*, 2010.

M. Owor, R. G. T Taylor, C. Tindimugaya, and D. Mwesigwa. Rainfall intensity and groundwater recharge: empirical evidence from the upper nile basin. *Environmental Research Letters*, 2009.

J. Poesen, F. Ingelmo-Sanchez, and H. Mucher. The hydrological response of soil surfaces to rainfall as affected by cover and position of rock fragments in the toplayer. *Earth Surface Processes and Landforms*, 1990.

Anders Rapp. Are terra rossa soils in europe eolian deposits from africa. *Geologiska Freningen i Stockholm Frhandlingar*, 1983.

P J Ribeiro and P J Diggle. geor: a package for geostatistical analysis. *R-NEWS*, 2001.

E. Shachnai. *Geological map of Israel, Sheet 8-IV*. Geological Survey Israel, 2000.

Roy C. Sidle, Shoji Noguchi, Yoshio Tsuboyama, and Karin Laursen. A conceptual model of preferential flow systems in forested hillslopes: evidence of self-organization. *Hydrological Processes*, 2001.

Arieh Singer. *The soils of Israel*. Springer, Heidelberg, 2007.

D. B. Stephens. Estimation of infiltration and recharge for environmental site assessment. *API Publ. 4643. Health and Environmental Sciences Department, Albuquerque, New Mexico*, 1996.

M. Tani. Runoff generation processes estimated from hydrological observations on a steep forested hillslope with a thin soil layer. *Journal of Hydrology*, 1997.

M. Weiler and J. McDonnell. Virtual experiments: a new approach for improving process conceptualization in hillslope hydrology. *Journal of Hydrology*, 2003.

Markus Weiler and Hannes Flühler. Inferring flow types from dye patterns in macroporous soils. *Geoderma*, 2004.

Menachem Weiss and Haim Gvirtzman. Estimating ground water recharge using flow models of perched karstic aquifers. *Ground Water*, 2007.

B. P. Wilcox, M. K. Wood, and J. M. Tromble. Factors influencing infiltrability of semiarid mountain slopes. *Journal of Range Management*, 1988.

D. H. Yaalon, Y. Nathan, H. Koyumdjisky, and J. Dan. Weathering and catenary differentiation of clay minerals in soils on various parent materials in israel. *Proceedings of the International Clay Conference Jerusalem*, 1966.

A. Yair. Hillslope hydrology water harvesting and areal distribution of some ancient agricultural systems in the northern negev desert. *Journal of Arid Environments*, 1983.